

Document NWPSAF-MO-TR-039

Version 1.0

02/03/20

NWP SAF AMV monitoring: the 9th Analysis Report (AR9)

James Cotton¹, Amy Doherty¹, Katie Lean², Mary Forsythe¹, Alexander Cress³

1. Met Office, UK
2. European Centre for Medium-Range Weather Forecasts (ECMWF)
3. Deutscher Wetterdienst (DWD)

NWP SAF AMV monitoring: the 9th Analysis Report (AR9)

James Cotton, Amy Doherty, Mary Forsythe (Met Office)

Katie Lean (ECMWF)

Alexander Cress (DWD)

This documentation was developed within the context of the EUMETSAT Satellite Application Facility on Numerical Weather Prediction (NWP SAF), under the Cooperation Agreement dated 7 December 2016, between EUMETSAT and the Met Office, UK, by one or more partners within the NWP SAF. The partners in the NWP SAF are the Met Office, ECMWF, KNMI and Météo France.

Copyright 2020, EUMETSAT, All Rights Reserved.

Change record			
Version	Date	Author / changed by	Remarks
0.1	12/12/19	J Cotton	First draft
0.2	16/01/20	J Cotton	Added content from Amy Doherty and Katie Lean
0.3	30/01/20	J Cotton	Feedback from Mary Forsythe and add summary
0.4	07/02/20	J Cotton	Add DWD inputs
0.5	12/02/20	J Cotton	Incorporate feedback from Roger Saunders
0.6	14/02/20	J Cotton / K Lean	Incorporate feedback from Katie Lean
1.0	02/03/20	M Forsythe	Version approved for publication

Contents

1. Introduction.....	2
2. Index of features identified in the monitoring.....	4
3. Impact of changes made by NOAA/NESDIS.....	10
4. Feature 9.1: Orographic impacts	12
5. Feature 9.2: Large vector differences near the South West African coast .	16
6. Feature 9.3: Differences between Met Office and ECMWF statistics for Himawari-8.....	24
7. Feature 9.4: EUMETSAT Metop low level AMVs in the winter hemisphere.	27
8. Update on Feature 5.2: Meteosat-8/11 negative bias during the Somali Jet	30
9. Update on Feature 8.1: Meteosat-8 (IODC) positive speed difference in the tropics	37
10. Summary	42
11. Acknowledgements.....	44
12. References	44

1. Introduction

The NWP SAF (Satellite Application Facility for Numerical Weather Prediction) Atmospheric Motion Vector (AMV) monitoring (<http://nwpsaf.eu/site/monitoring/winds-quality-evaluation/amv>) provides tools to monitor, document and investigate error characteristics of AMV data.

The NWP SAF provides a long-term archive of observation-minus-background (O-B) statistics where the AMVs are compared with short-range forecasts from an NWP model. Forecast model fields are interpolated in time and space to the observation location and used to calculate a model-equivalent of the observation, referred to as the “background” value. O-B are calculated against both Met Office and ECMWF global models, to give insight into whether features seen in the monitoring are related to problems with the models or with the AMVs.

An extensive set of AMV products are actively monitored by the NWP SAF (Table 1). Previous generations of satellite/instruments can also be found in the archive. New data sets added to the monitoring since 2018 are Meteosat-11, GOES-16/17, INSAT-3DR, NOAA-20 and Metop-C (Table 2).

Analysis reports are released at intervals of 2-years to help guide discussion on improvements to the AMV derivation and assimilation. Results are presented at the workshops of the International Winds Working Group (IWWG). The analysis reports identify features from the monitoring statistics and document how these evolve over time. Where possible attempts are made to diagnose the cause of the difference between the AMVs and the model.

This paper marks the ninth in the series of analysis reports (AR9). Previous analysis reports are hereafter referred to by the order of their publication e.g. 8th Analysis Report (AR8), 7th Analysis report (AR7), etc, and are available to download from the website.

The paper is structured as follows. Section 2 provides a status summary of the current active features in the monitoring and any new features in AR9. Section 3 describes the impact of changes made by NOAA/NESDIS to the GOES AMVs.

New features investigated in AR9 are:

Feature 9.1: Orographic impacts,

Feature 9.2: Large vector differences near the South West African coast,
 Feature 9.3: Differences between Met Office and ECMWF statistics for Himawari-8,
 Feature 9.4: EUMETSAT Metop low level AMVs in the winter hemisphere.
 These are shown in Sections 4, 5, 6, and 7 respectively.

Updates are provided on two existing features in Sections 8 and 9:

Update on Feature 5.2: Meteosat-8/11 negative bias during the Somali Jet

Update on Feature 8.1: Meteosat-8 (IODC) positive speed difference in the tropics.

Finally, a brief summary is provided in Section 10.

Geostationary AMVs	Producer	Channels
Meteosat-8/10/11	EUMETSAT	IR 10.8, WV 6.2, WV 7.3, VIS 0.8, HRVIS
Himawari-8	JMA	IR, WV 6.2, WV 6.7, WV 7.3, VIS
GOES-15/16/17	NOAA/NESDIS	IR, SWIR, WV, VIS
INSAT-3D/3DR	ISRO	IR, SWIR, WV, VIS
COMS-1	KMA	IR, SWIR, WV, VIS
FY-2E/G	CMA	IR, WV
Leo AMVs		
Terra	NESDIS, DB	IR
Aqua	NESDIS, DB	IR, WV, CSWV
NOAA-15/18/19	CIMSS, DB	IR
Metop-A/B	EUMETSAT, CIMSS	IR
Metop-C	EUMETSAT	IR
Suomi NPP	NESDIS, DB	IR
NOAA-20	NESDIS	IR
Mixed AMVs		
LeoGeo	CIMSS	IR
Dual-Metop	EUMETSAT	IR
Stereo Motion Vectors		
Terra MISR	NASA-JPL	VIS

Table 1. AMV datasets monitored by the NWP SAF. Channels are infrared (IR), short wave infrared (SWIR), visible (VIS), high resolution visible (HRVIS), cloudy water vapour (WV), clear sky water vapour (CSWV). DB stands for direct broadcast station.

Change	Type	Date available	Description
GOES-16	Transition	Jan 2018	GOES-16 replaced GOES-13 as GOES East
Meteosat-11	Transition	Feb 2018	Meteosat-11 replaced Meteosat-10 as the 0° service
Meteosat-10	Transition	Mar 2018	Meteosat-10 replace Meteosat-9 as the rapid scan service
Metop-C	New	Feb 2019	Metop-C added
GOES-17	New	Jun 2019	GOES-17 added in parallel with GOES-15
NOAA-20	New	Oct 2019	NOAA-20 added
INSAT-3DR	New	Nov 2019	INSAT-3DR added

Table 2. Changes to monitoring since 2018.

2. Index of features identified in the monitoring

Table 3 documents the features that were active from AR8 and provides an update on their current status within the monitoring. In some cases, features may have been renamed from previous reports to better reflect the pattern or cause. Newly identified features are also listed. For each feature, the table indicates whether further details are provided in the following sections of this report.

Features are referenced in the format X.Y, where X is the number of the analysis report where that feature was first described, and Y is the example number.

Unless otherwise specified, the tropics refer to the area 20°N-20°S and the extra-tropics polewards of these boundaries. Upper-level, mid-level and low-level refer to AMV heights above 400 hPa, between 400-700 hPa and below 700 hPa respectively.

Table 3. Status of the active features identified in the AMV monitoring. Green shading denotes a new feature, blue denotes a feature than is fixed or considered closed. The AR column lists the analysis report numbers where that features is discussed. The AR9 column shows whether a feature is discussed further in this report.

Ref. number	Feature name	AR	Status	AR9
Geostationary: low-level (below 700 hPa)				
2.3	GOES winter negative bias over NE America	2,3,6	Still present. Feature background: AR3 highlighted observations over land with a high height bias relative to the level of best-fit. This was linked to low level winds assigned to cloud base over sea, but not over land. AR6 showed a negative bias is also observed over N. Atlantic during cold air outbreaks which is linked to model forecast bias and difficulties in tracking the breakup of cloud along the SST front.	
2.6	Meteosat-8/11 positive bias over N Africa	2,3,4,6	Still present. Feature background: A large positive wind speed bias is observed in the Meteosat Second Generation (MSG) IR and visible channels over North Africa and the Arabian Peninsula during winter. Although mainly over land, the bias does extend over the Atlantic to the west of Africa in January/February and moves northwards into the Mediterranean by May. AR4 linked the bias to large height assignment errors when tracking cirrus clouds, leading to very fast winds being assigned around 500 hPa too low. The feature closely matches the location of the sub-tropical jet stream. Investigated positive biases over Arabian Peninsula in July 2018 and July 2019. Case for 27 July 2018. IR channel shows AMVs are easterlies whereas background is west or north-westerlies. Observed pressures are typically 700-800 hPa, best-fit is 100-200 hPa. Imagery shows tracking thin cirrus moving from east to west. Appears to be a classic example of large height assignment error. Also noted lots of dust in the imagery but AMVs (600-700 hPa) for this appear to match the model well.	
2.7	Spuriously fast Meteosat and MTSAT winds	2,3,4,6,7	Closed. Satellites no longer active.	
4.1	Model differences in the Pacific	4,5	Closed. Models now more consistent.	
5.1	Patagonia negative bias	5	Closed. No longer present following the change from GOES-13 to GOES-16.	
5.2	Meteosat-8/11 negative bias during Somali jet	5,6	Still present – see update.	Y

			Feature background: SEVIRI AMVs from Meteosat-8 and Meteosat-11 show a large negative wind speed bias during July and August in the NW Indian Ocean, near the Gulf of Aden. This time period coincides with the strengthening of the Somali Low-Level Jet. Previous investigation has shown the bias is due to instances of height assignment error, with slow upper level vectors incorrectly assigned within the fast, low-level wind regime, and the influence of an island (Socotra) causing semi-stationary wave cloud formations within the jet.	
6.1	Bias in tropical E Atlantic	6	Closed. Much less prominent.	
6.2	FY-2E/G bias during NE winter monsoon	6	Renamed as not seen for Himawari-8 (was in MTSAT). Feature background: a marked negative speed bias in the northern hemisphere during the winter months from November to March. AR6 indicates that the negative-biased observations may have been assigned too high.	
8.1	Meteosat-8 (IODC) positive speed difference in the tropics	8	Still present - see update. Feature background: Meteosat-8 low level winds show a positive speed O-B and high RMSVD over the southern tropics of the Indian Ocean. Model and radiosonde profiles provide evidence for a lack of shear in the AMVs which leads to a positive speed bias above 900 hPa height. Best-fit pressure indicates this could be due to AMVs being assigned too high.	Y
9.2	Large vector differences near the South West African coast	new	Meteosat-10 and Meteosat-8 low level IR winds show an area of large vector differences along the Atlantic coast of Southern Africa.	Y
Geostationary: mid-level (400-700 hPa)				
2.8	Positive bias in the tropics for MSG, FY-2, COMS	2,3,4,5,6,7	Renamed to reflect satellites affected. Feature background: Previous reports have noted that mid-level AMVs tended to have a positive speed bias in the tropics and a negative speed bias in the extra-tropics. As new generations of satellites and derivation schemes have been introduced this has no longer been the case, e.g. for Himawari-8, and GOES-16/17. In general, there are far fewer AMVs extracted at mid-level and biases are thought to be largely the result of height assignment errors.	
2.9	Negative bias in the extra-tropics for MSG, FY-2	2,3,4,5,6,7		
Geostationary: high-level (above 400 hPa)				

2.10	Negative speed bias in extra-tropics for MSG, FY-2 and COMS	2,3,4,5,6	<p>No longer valid for Himawari and GOES. Renamed to reflect satellites affected.</p> <p>Meteosat-11: Still prominent in IR, less in WV7.3 and less again in WV6.2 (difference between channels). In July 2018 there is a marked negative bias in all 3 channels around 30-60E, 40-50N which is not in an area of high wind speeds.</p> <p>Meteosat-8: Almost semi-permanent area of negative bias over Asia which appears to mark the position of the Himalayan Plateau. See new feature on orographic effects.</p> <p>FY-2G: Strong negative bias in IR.</p> <p>Himawari-8: IR and WV7.3 neutral. WV6.2 has general slight positive bias.</p> <p>COMS: Strong negative bias.</p> <p>GOES-16: IR and WV positive bias improved since November 2018. See update on NESDIS changes in section 3.</p>
2.13	Positive speed bias in tropics for MSG and FY-2	2,3,4,5,6,7	<p>Renamed to reflect satellites affected.</p> <p>Meteosat-8/11: Positive bias still present.</p> <p>GOES-16: A small area of marked positive bias in February 2019 near Central America.</p> <p>FY-2G: Positive bias in IR, less so in WV.</p> <p>Himawari-8: IR and WV7.3 neutral. WV6.2 has a general slight positive bias but not specific to tropics.</p>
2.14	High troposphere positive bias	2,3,6	<p>Still present in MSG (previously shown in AR8 to be better in OCA) and unedited GOES.</p> <p>Feature background: A positive speed bias for MSG and GOES (unedited data) AMVs assigned heights high in the upper troposphere. The bias may be due to a 'high' height assignment bias. There is a seasonal dependence affecting the EUMETSAT data: a positive bias can be observed between October-April, the rest of the year is dominated by a negative speed bias.</p>
2.15	Differences between channels	2,3,5	Zonal plots suggest there are still difference between IR and WV channels for MSG, GOES-16 and Himawari-8.
3.2	Negative Speed bias in Tropical Easterly Jet (TEJ)	3,6	<p>Zonal plots for Met-8 IR for August 2018 shows this is likely still a problem as the bias versus the Met Office is larger than versus ECMWF.</p> <p>Feature background: A negative speed bias for Meteosat-7 and MSG winds in the high-troposphere of the tropics between June and September. Previously shown to be contribution from Met Office model error linked to an excessive TEJ in the analysis.</p>
4.2	GOES negative bias in tropical Pacific	4,5,6	Still present for GOES-15 and slightly worse for Met Office compared to ECMWF (GOES-17 data available from late March so not able to investigate).

			Feature background: GOES West exhibits a negative speed bias from December to April. Model errors are thought to contribute to the O-B signal which has also previously been shown to vary from year to year indicating some synoptic dependence.	
5.3	MTSAT tropical cyclone speed bias	5,6,7	Closed. Not seen in Himawari-8.	
9.5	Negative speed bias in tropics for GOES-16/17	new	January 2019 and February 2019 are recent examples where there is a pronounced negative bias in both IR and WV channels. Biases are somewhat reduced following change in November 2018 (see update on NESDIS changes in section 3).	Y
Leo and mixed AMVs				
2.19	Aqua WV high-level positive speed bias	2,3,4,5	Still present for Aqua WV, not really in other data sets. Feature renamed to reflect this.	
2.20	Low-level negative speed bias	2,3,4	Still present in CIMSS AVHRR and NESDIS MODIS. Not apparent in NPP.	
4.3	Near-pole mid-level negative bias 4,5	4,5	More of a general negative bias for CIMSS and MODIS winds.	
6.4	EUMETSAT Metop near the poles	6	Closed. A bullseye pattern bias in the Mid-level EUMTSAT AVHRR product was reported in AR6. It is no longer seen and has not been seen consistently since April 2014. In May 2014 the EUMETSAT Metop AVHRR Polar Winds algorithm was updated to version 2.3.3 with reduced RMSVD and bias against forecast, which may account for the improvement (ref EUMETSAT, 2019)	
7.1	Dual-Metop high level positive bias in tropics	7	Improved bias, MVD and increased numbers from January 2019, not just in the tropics. This coincides with the introduction of Metop-C in the dual-Metop product. The drift of the Metop-A orbit as it nears end of life had been reducing the number of winds. Details from EUMETSAT user support email dated 21 January 2019, " <i>Changes to production rules of dual-Metop AMV products</i> ": As of 17 January 2019, dual-Metop winds are A/B, B/C and C/A pairs. The generation of B/A winds was ceased because of the degraded quality and the lower number of winds. The new setup reduces the time gap between the image pairs to about 30-35 minutes which improves the product coverage and wind quality. It has been noted that there are differences in the characteristics between the A/B pair and the two other pairs B/C and C/A (Borde et al, 2019). The A-B pair presently has the worst overlap, with the largest differences in the viewing geometries. C-A has the best overlap and the most similar viewing geometries. BC is somewhere in-	

			between. The geometry is important as the AVHRR pixel size varies from 1km at nadir to 4km at the edge of the swath.	
7.2	EUMETSAT Metop high level negative bias in midlatitudes	7	Still present. Some improvement in Dual-Metop due to change mentioned in 7.1. Feature background: A negative speed bias affecting single and dual Metop winds between 20-20 degrees latitude at upper levels.	
7.3	MISR positive bias over ice and desert	7	Still present. Feature background: MISR often shows a positive speed bias and large mean vector difference at low level over ice and desert. The low heights are believed to be due to tracking cloud shadows rather than the clouds themselves. Since the shadows have no apparent north-south motion due to parallax as is seen for clouds, they are assigned heights very close to the surface.	
7.4	LeoGeo coverage gaps at particular longitudes	7	Closed. Coverage improved since GOES-16 added in January 2018.	
7.5	MISR bad orbits	7	Still present. Feature background: Monitoring of MISR AMVs often reveals stripes of data with large O-B differences. These are usually over the Atlantic or Pacific oceans. MISR winds retrieval requires visible landmarks to calibrate its camera geometry. The near-real time MISR winds processing is done with 10-50 minute data sessions. A session's data quality can be degraded if the Terra satellite does not pass over enough land to calibrate its cameras during that session.	
7.6	VIIRS square distribution	7	Still present in NPP and the same for NOAA-20. Coverage in restricted by a hard limit used to define the box size for the polar projection during the derivation process	
9.4	EUMETSAT Metop low level AMVs in winter hemisphere	new	Metop low level winds have a speed bias and large vector difference in the winter hemisphere	Y
General issues				
9.1	Orographic effects	new	Meteosat-8 has almost semi-permanent area of negative bias over Asia which appears to mark the position of the Himalayan Plateau. Apparent in all 3 channels and all year, apart from JJA. Not seen in Himawari (just about has coverage), INSAT or in dual Metop.	Y
9.3	Differences between Met Office and ECMWF statistics for Himawari-8	new	ECMWF has smaller mean vector differences at upper levels, Met Office has smaller mean vector differences at mid-level in tropics. Differences also in biases at mid-level.	Y

3. Impact of changes made by NOAA/NESDIS

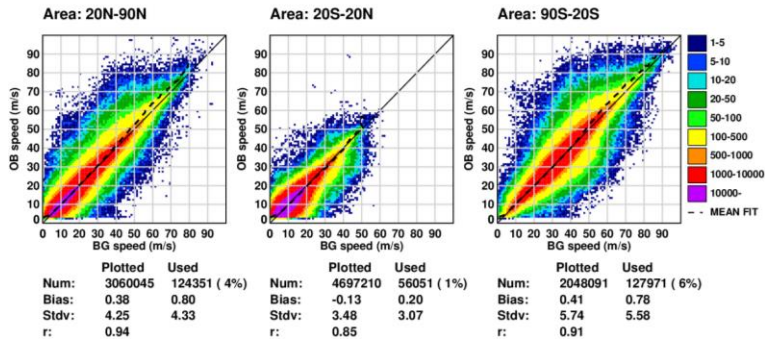
Since AR8, NOAA/NESDIS have made two changes which have impacted the GOES AMVs and these are observed in the NWP SAF monitoring.

- 1) An updated internal quality control check was implemented in October 2018. This checks the AMVs for gross errors versus the GFS model forecast using channel-dependent vector difference thresholds, e.g. 6 ms^{-1} for visible, 10 ms^{-1} for IR 11.2μ winds (see Daniels et al., 2018). The impact of the change can be clearly seen in the 2D histograms as a narrowing of the wind speed O-B distribution resulting in reduced standard deviations (Figure 1). Map and zonal plots of mean vector differences also show a strong reduction following the change. For example, GOES-16 visible channel AMVs showed a positive speed bias over land for the western portion of North America up until September 2018 (Figure 2, left). Following the implementation of the gross error check, the bias and most of the AMVs in this area are removed and the O-B over land are generally reduced everywhere (Figure 2, right).
- 2) GOES-16 and GOES-17 Advanced Baseline Imagers (ABI) have been operating in Mode 6 since 2 April 2019. This mode provides a full disk image every 10 mins (previously 15 mins), although the AMV products themselves remain hourly. The change to 10-minute imagery impacted the number of visible AMVs the most, roughly doubling the counts. There are some additional winds from other channels, but less dramatic. Note that the change to Mode 6 has helped fill in the coverage gaps in the visible channel winds introduced by the gross error change mentioned in 1) over North America.

A further planned change announced at IWW14 has yet to be implemented. The use of an updated cloud height algorithm to improve the AMV height assignment (and hence speed biases) at upper levels has been delayed.

The monthly monitoring plots also show a change in the spatial distribution of the GOES-16 visible winds between November and December 2018 (Figure 3). In the South Pacific Ocean, the number of winds appeared truncated south of 30°S but after the change there are far more vectors available. The reason for the change is unknown.

GOES-16 IR, September 2018, Above 400 hPa



GOES-16 IR, November 2018, Above 400 hPa

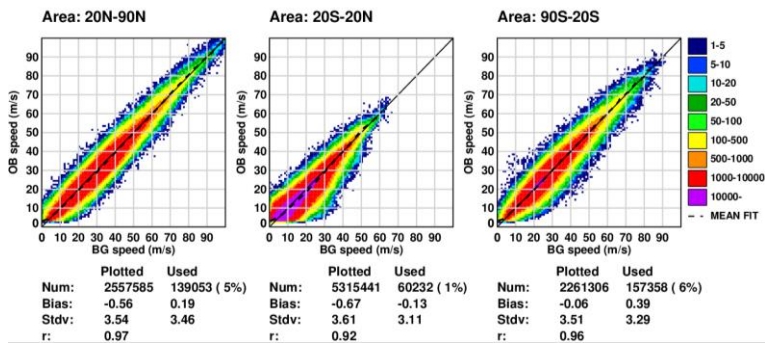


Figure 1. 2D histograms of AMV versus model background wind speed for GOES-16 IR channel winds in September 2018 (top) and November 2018 (bottom). Data after filtering for QI2 > 80 for high-level winds. Histograms are separated according to latitude band.

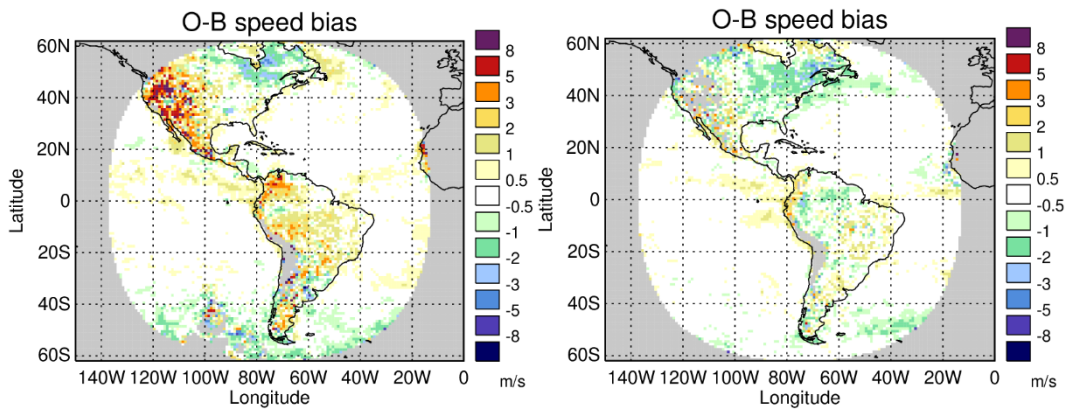


Figure 2. Map of O-B speed bias for GOES-16 visible channel AMVs below 700 hPa height in August 2018 (left) and November 2018 (right).

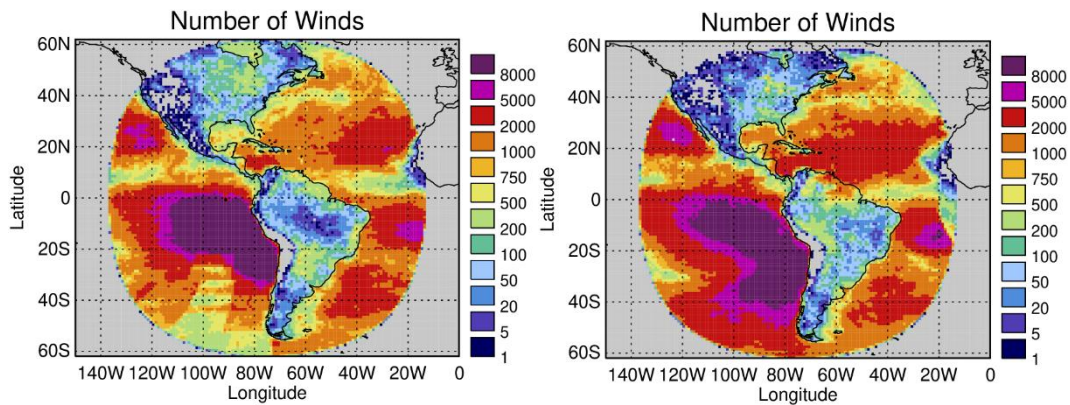


Figure 3. Map of AMV counts for GOES-16 visible winds below 700 hPa height in November 2018 (left) and December 2018 (right).

4. Feature 9.1: Orographic impacts

Meteosat-8 has an almost semi-permanent area of negative bias over Asia which coincides with the position of the Himalayan Plateau. Here we consider the impact of orography (surface height) on AMV departures more widely to see if other AMV data sets are also affected. Note that the various AMV data sets compared have different spatial sampling of high land

SEVIRI AMVs from Meteosat-8 have the largest sensitivity to orography. IR and cloudy WV AMVs from Meteosat-8 show an increasing negative wind speed bias for increasing model surface height and this effect is largest for AMVs with higher pressures, i.e. those closer to the surface (Figure 4, 1st row). GOES-16 IR and WV channel AMVs show similar trends to SEVIRI (Figure 4, 2nd row) but the magnitudes of the wind speed bias are much smaller than those seen for Meteosat-8. Over high land surfaces Himawari-8 AMVs have a small, increasing positive wind speed bias, which is largest for AMVs assigned to the lowest pressures (Figure 4, 3rd row). Like SEVIRI, the EUMETSAT dual Metop winds also have a negative wind speed bias for increasing model surface height (Figure 4, 4th row), but the magnitude of the bias is much reduced. Polar winds from Suomi-NPP, NOAA-19 and EUMETSAT Metop-B show little sensitivity to model orography, apart from data over land above 4 km (Figure 4, 5th row).

For Meteosat-8, coverage of high land surfaces is predominantly the Himalayas and the Tibetan Plateau and this coincides with an area of strong negative speed bias for IR and cloudy WV AMVs (Figure 5). Maps from the NWP SAF website show the wind speed bias over the Himalayan plateau is present for most of the year between October and May, but not in northern hemisphere summer (JJA).

Other data sets which cover the Himalayan Plateau include Himawari-8 and dual Metop. Himawari-8 shows good agreement with the model winds. The dual Metop AVHRR winds show a negative bias over the Himalayas but only for AMVs assigned to mid-level. It has been previously noted that this area has caused problems for FY-2 AMVs (see update under Feature 2.10 in AR6).

Direct comparison of Meteosat-8 with dual Metop and Himawari over the Himalayan Plateau area reveals good agreement in the derived motions. The comparison of assigned heights however, shows that Meteosat-8 vectors are assigned around 40-50 hPa higher in height than dual Metop and Himawari in both winter and summer (Figure 6). The consistent nature of the height difference suggests the absence of the negative speed bias in northern hemisphere summer is due to changes in the wind regime. In January the maximum wind speed is much greater, as is the upper layer vertical wind shear (Figure 7). For Meteosat-8, a 50 hPa error in height produces a much larger error in wind speed in January than in July (Figure 7, left). By comparison, the Himawari-8 profiles are very similar to the model (Figure 7, right).

In summary, Meteosat-8 shows the largest impact due to high land surfaces and this occurs mainly over the Himalayan Plateau. We find a strong negative speed bias for most of the year, except in northern hemisphere summer. In both summer and winter there is a consistent 50 hPa height difference between Meteosat-8 and other AMVs in this area. This height bias has less of an impact in summer when the vertical wind shear is less.

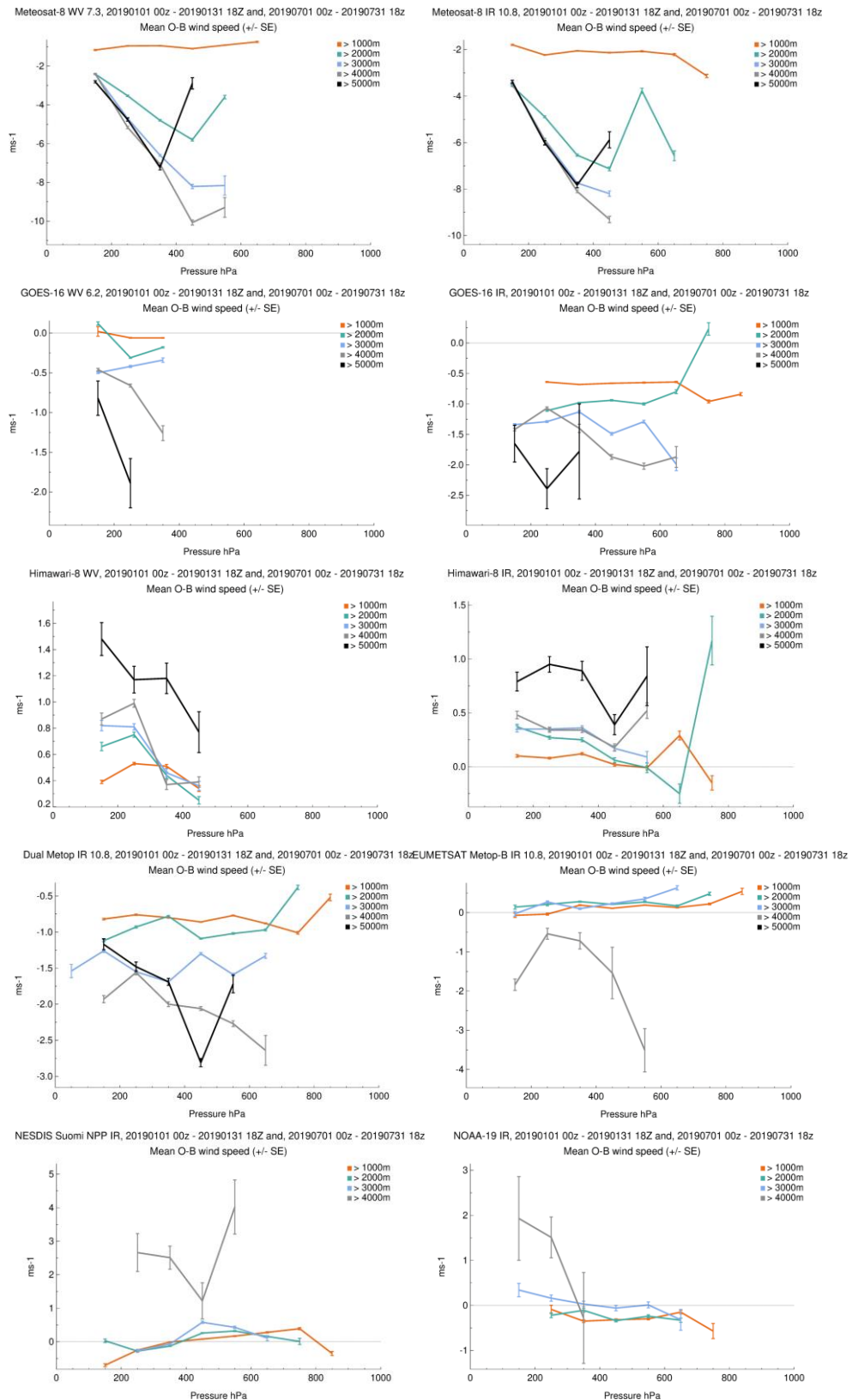


Figure 4. Mean O-B wind speed as a function of AMV pressure level separated by model orography: land heights over 1 km (red), 2 km (green), 3 km (blue), 4 km (grey) and 5 km (black). Meteosat-8 (1st row), GOES-16 (2nd row), Himawari-8 (3rd row), EUMETSAT dual Metop and single Metop-B (4th row), Suomi-NPP and CIMSS NOAA-19 (5th row).

Met Office: Meteosat-8 IR 10.8 All Lev, January 2019

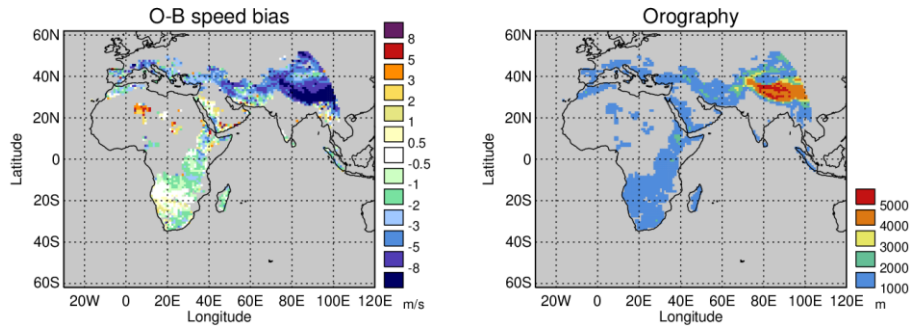


Figure 5. Mean O-B wind speed (left) and model orography (right) for Meteosat-8 IR10.8 channel AMVs located above land greater than 1 km high. Data for January 2018 and QI2 greater than 80.

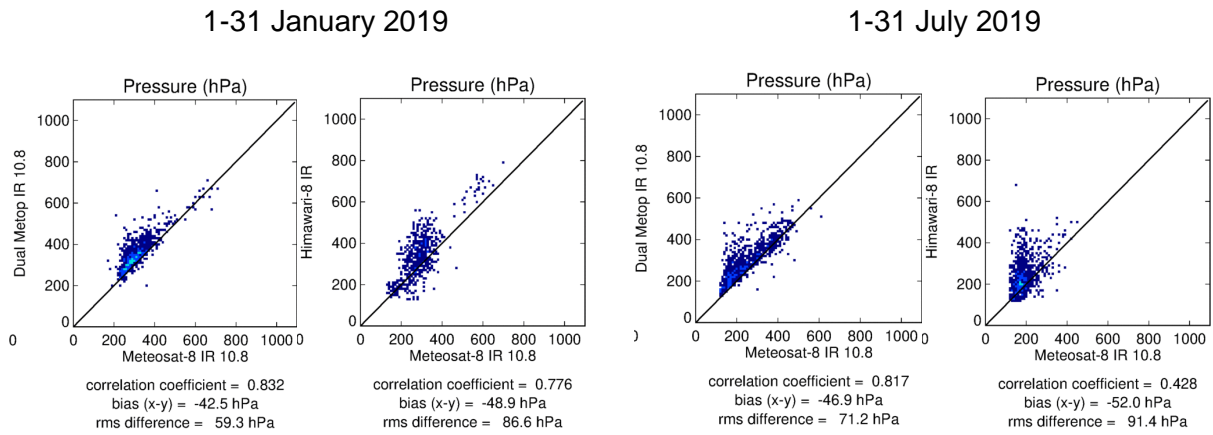


Figure 6. Height comparison of Meteosat-8 IR 10.8 channel AMVs with Dual Metop and Himawari-8 over the Himalayan Plateau area. Selected AMVs for model orography greater than 1 km, located within box 20-40N, 70-105W. The matchup criteria are AMVs within 10 km and 30 mins. The comparison is performed for January 2019 (left image pair) and July 2019 (right image pair).

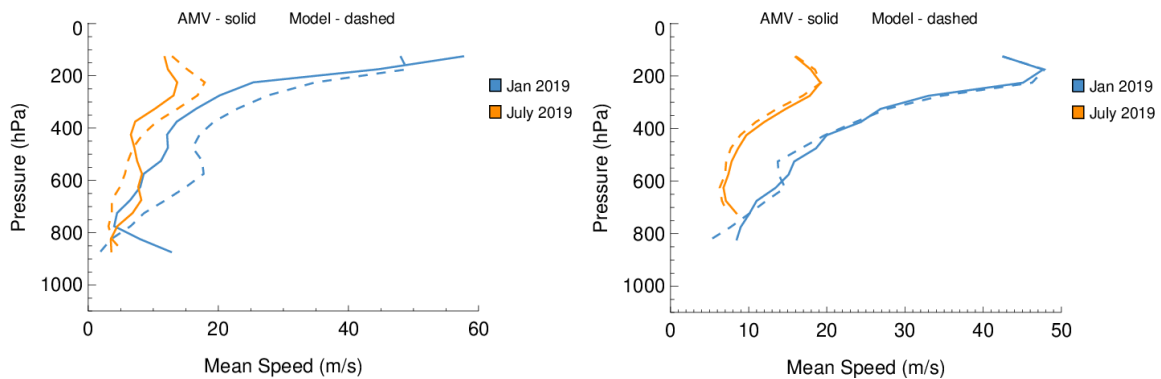


Figure 7. Profiles of mean AMV wind speed (solid line) and mean background wind speed (dashed line) for Meteosat-8 IR10.8 channel (left) and Himawari-8 IR (right). Data shown for January 2019 (blue) and July 2019 (orange). Selected AMVs for model orography greater than 1 km, located within box 20-40N, 70-105W and QI2 > 80.

5. Feature 9.2: Large vector differences near the South West African coast

Meteosat-10 and Meteosat-8 low level IR winds show an area of large vector differences along the Atlantic coast of Southern Africa. This feature is present for several months each year but does not appear in the winter months of June and July. It is most apparent in the IR channel, but is also seen to some extent in the high-resolution visible channel.

The feature is characterised by large mean and RMS vector differences (Figure 8), with systematic O-B components originating from a positive wind speed bias and a negative wind direction bias. The mean model flow is a south easterly, whereas the mean AMV flow has more of a north/westerly component. Mean observed minus best-fit pressure differences are over +200 hPa along the coast zone indicating the AMVs are possibly assigned too low according to the model wind profile.

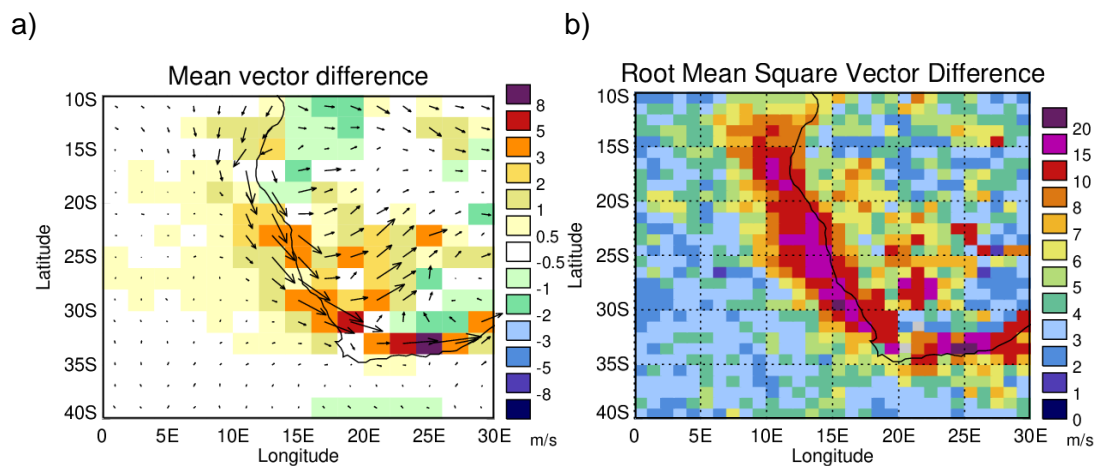


Figure 8. Meteosat-11 IR10.8 AMVs assigned below 700 hPa height in May 2019. a) Mean O-B vector difference (arrow) and mean O-B speed bias (colour shading), b) root mean square vector difference.

The month of May 2019 is selected for further investigation. Hovmoeller plots over the region of interest (15S-35S, 5E-20E) show that large RMS and mean vector differences frequently occur for AMVs assigned heights around 960 hPa, but there are periods of several days where the model and the observations do show better agreement.

Case study

To view an animation of the AMVs and imagery discussed in this case study, please visit the following link:

https://nwpsaf.eu/monitoring/amv/animations/m11ir108_20190505T2100Z_20190506T2100Z.gif

We use the 00 UTC – 18 UTC cycles on the 6 May 2019 as an example of where large vector differences occur in this region. Meteosat-11 IR AMVs and image data valid at 2330 UTC on

5 May show a ribbon of upper level cloud over the South Atlantic moving from north west to south east (Figure 9). The majority of AMVs tracking this cloud have wind speeds around 40 ms^{-1} , are assigned pressures in the range 230-400 hPa and show good agreement with collocated model wind directions. However, one vector of 40 ms^{-1} has been assigned as low as 960 hPa where the model is a south/south-easterly of around 5 ms^{-1} , leading to a huge O-B vector difference. Further examples can be seen further north (AMVs around 9°E , 20°S) where high level westerlies have been assigned to 960 hPa. It is clear from the imagery that the upper level clouds in this area are running over a sheet of low cloud, so it is possible the Cross Correlation Contribution (CCC) height assignment has been based on the wrong pixels in this multi-layer cloud scenario. Another possibility is that the input cloud top height product, in this case from Cloud Analysis (CLA), is incorrect.

We additionally monitor Meteosat-11 AMVs assigned heights using the Optimal Cloud Analysis (OCA). The vector tracking the ribbon of high cloud is assigned to 960 hPa with CLA but assigned 277 hPa with OCA, much closer to model best-fit pressure at 234 hPa. The fast westerly AMVs assigned to 960 hPa further north are no different with OCA. However in general, AMVs assigned CLA heights of 960 hPa are often assigned much higher heights between 200-600 hPa with OCA (Figure 10).

The sheet of fog or low cloud that stretches along the Namibian coast also appears to cause large O-B differences in a more direct way. AMVs located near 21°S , 12.6°E appear to be tracking low cloud and are assigned to 960 hPa but have north-easterly wind directions roughly perpendicular to the model (south-easterly) and slower wind speeds. Two AMVs with similar discrepancies are also seen near 16°S , 10°E . Nearby AMVs which appear to track the same low cloud, are south-easterlies at 960 hPa and these show good vector agreement with the model (best-fit pressure 980-1000 hPa). So why are some AMVs tracking easterlies in this area? To better understand what is happening we move forward and consider data valid at 0630 UTC on 6 May (Figure 11). IR imagery now shows a gap in the bank of low cloud, with a well-defined rear edge to the western portion. Sequences of images show this rear edge is indeed moving in a north-easterly to south-westerly direction and the north-easterly AMVs are tracking this motion. It is possible there is a second layer of cloud and that the AMV heights are simply assigned too low, as model best-fit pressure suggests around 700 hPa. It may also be that the movement of the rear edge of this cloud is not representative of the local wind, i.e. it is breaking the passive tracer assumption.

From around 0630 UTC onwards the banks of fog or low cloud along the coastline and just inland begin to burn back towards the coast and dissipate with the heat of the day. The cloud

with the defined rear edge also appears to then be advected away with the south-easterly flow as it dissipates.

Data valid at 1330 UTC shows that much of the coastline is free of low cloud (Figure 12). Some large height assignment errors remain for the ribbon of high cloud moving off the Atlantic. Vectors located between 24°S-27°S and assigned to 960 hPa have model best-fit pressures near 500 hPa. Two nearby vectors assigned to 500-600 hPa agree better with the model. For the winds assigned to 960 hPa with CLA, the same vectors with OCA are assigned around 350-400 hPa (Figure 13). Both findings suggest the vectors at 960 hPa are assigned far too low. This is validated by a Calipso overpass at ~1328 UTC (Figure 14) which shows:

- I. Mid-high clouds south of 24°S with cloud top heights in the range 6-7 km (~490-430 hPa) and 8-9 km (~380-330 hPa). Although some of the signal is attenuated, there is a layer of low cloud and aerosol below 1 km (>900 hPa).
- II. High cloud north of 24°S with cloud tops around 13-15 km (180 – 130 hPa). This is overlying a layer of low cloud with cloud tops below 1 km. This is likely the low cloud being advected away with the south-easterly flow as described above. Note there is no sign of any cloud layers near 700 hPa (~ 3km).

In summary, the case study indicates there are at least two causes for the large O-B vector differences in this region. Firstly, AMVs tracking high clouds which are incorrectly assigned to 960 hPa. A Calipso overpass shows this occurs in a multi-layer cloud scenario and image sequences suggests this to be quite common due to the prevalence of low cloud in the area. AMVs assigned heights with OCA are often much improved in these situations. Secondly, a well-defined break in the fog or low cloud shows an apparent motion perpendicular to both the model and other near AMVs assigned to 960 hPa. Model best-fit pressure for the north-easterly AMVs is around 700 hPa but Calipso fails to show any cloud layers at this height. It is possible that the motion of the cloud break is not representative of the local wind. The monthly O-B variations observed in the monitoring, notably the reduction in vector differences in June and July, can be explained by the seasonal variations in fog and low cloud in this area. Cermak (2012) shows the frequency of fog and low cloud along the south-western African coast is highest in summer and lowest in June.

AMV m11ir108 20190505T2300Z - 20190506T0000Z
SEVIRI 20190505 2330 UTC infrared 10.8 micron

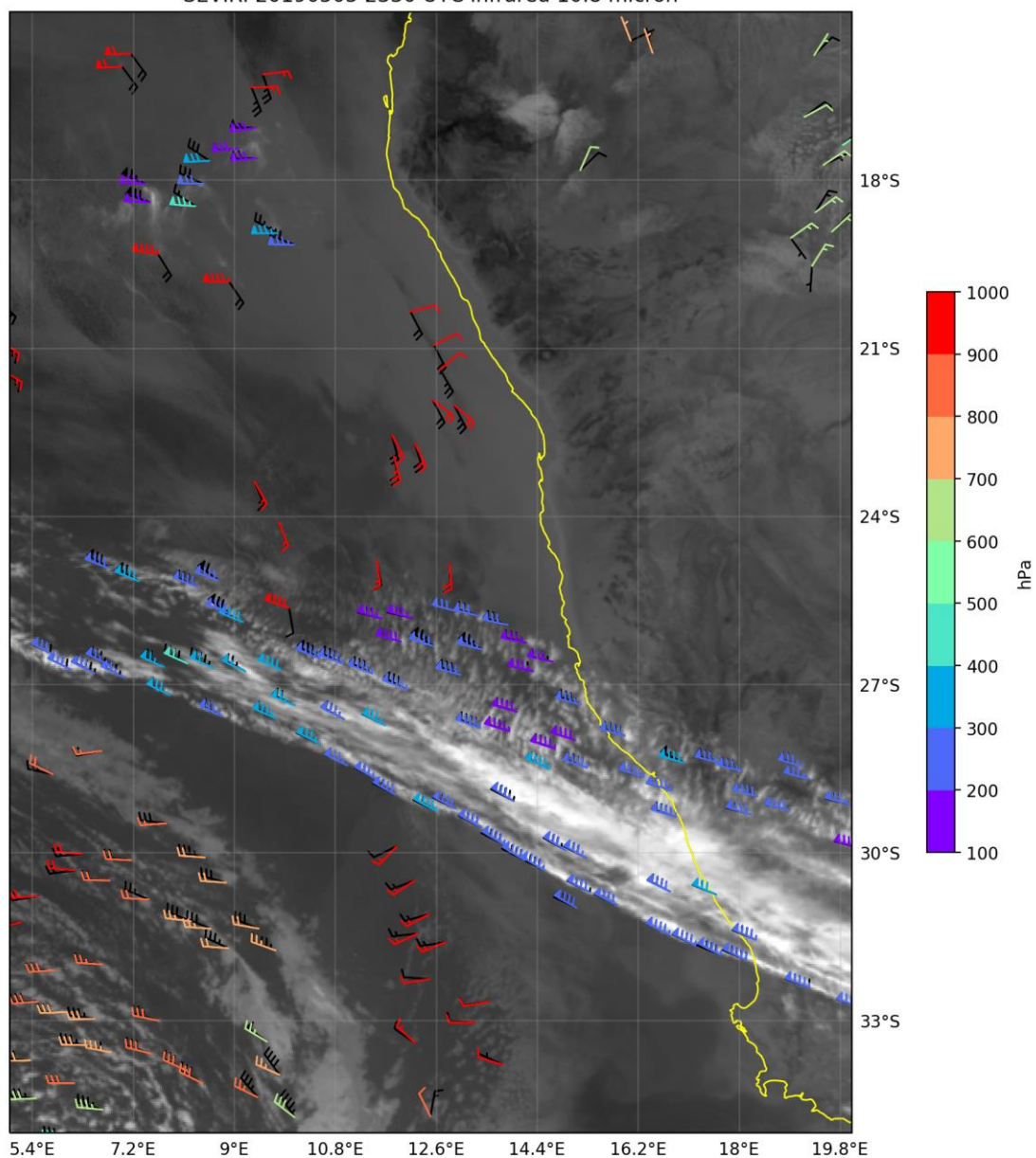


Figure 9. Meteosat-11 IR 10.8 μ m image and AMVs valid at 2330 UTC on 5 May 2019. AMVs are filtered for QI2 > 80 and colours represent the assigned AMV height (pressure) band. Collocated model background winds are shown in black. Half barbs, full barbs and flags represent wind speeds of 2.5 ms^{-1} , 5 ms^{-1} and 25 ms^{-1} respectively.

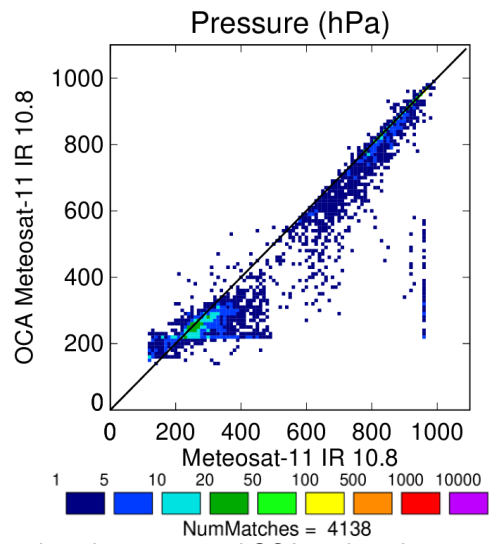


Figure 10. Comparison of CLA assigned pressure and OCA assigned pressure for Meteosat-11 IR10.8 AMVs. Data valid for 00-18 UTC cycles on 6 May 2019 and filtered for QI2 > 80, latitude bounds 35S-15S and longitude bounds 5E-20E.

AMV m11ir108 20190506T0600Z - 20190506T0700Z
SEVIRI 20190506 0630 UTC infrared 10.8 micron

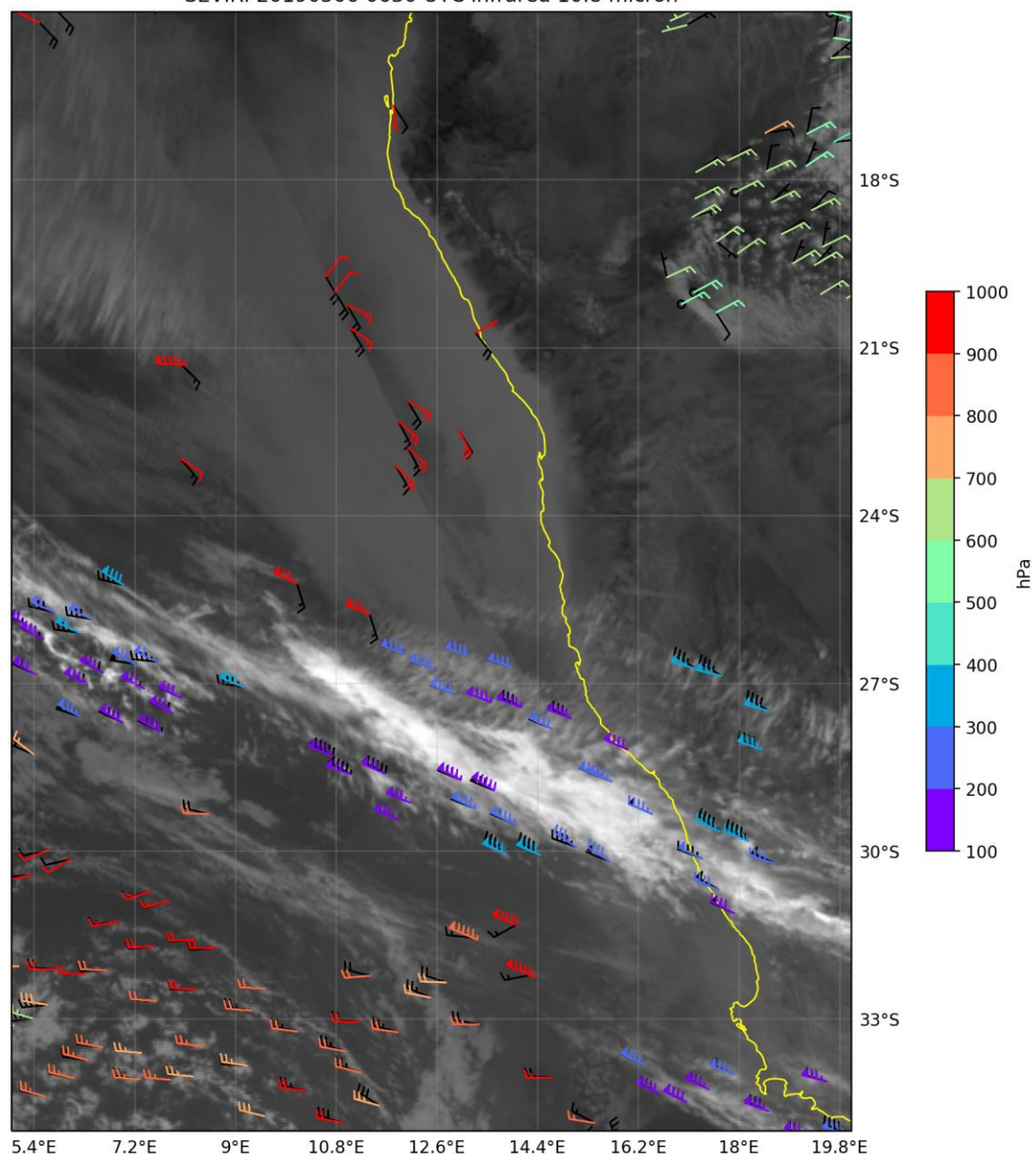


Figure 11. Same caption as Figure 9, but for data valid at 0630 UTC on 6 May 2019.

AMV m11ir108 20190506T1300Z - 20190506T1400Z
SEVIRI 20190506 1330 UTC infrared 10.8 micron

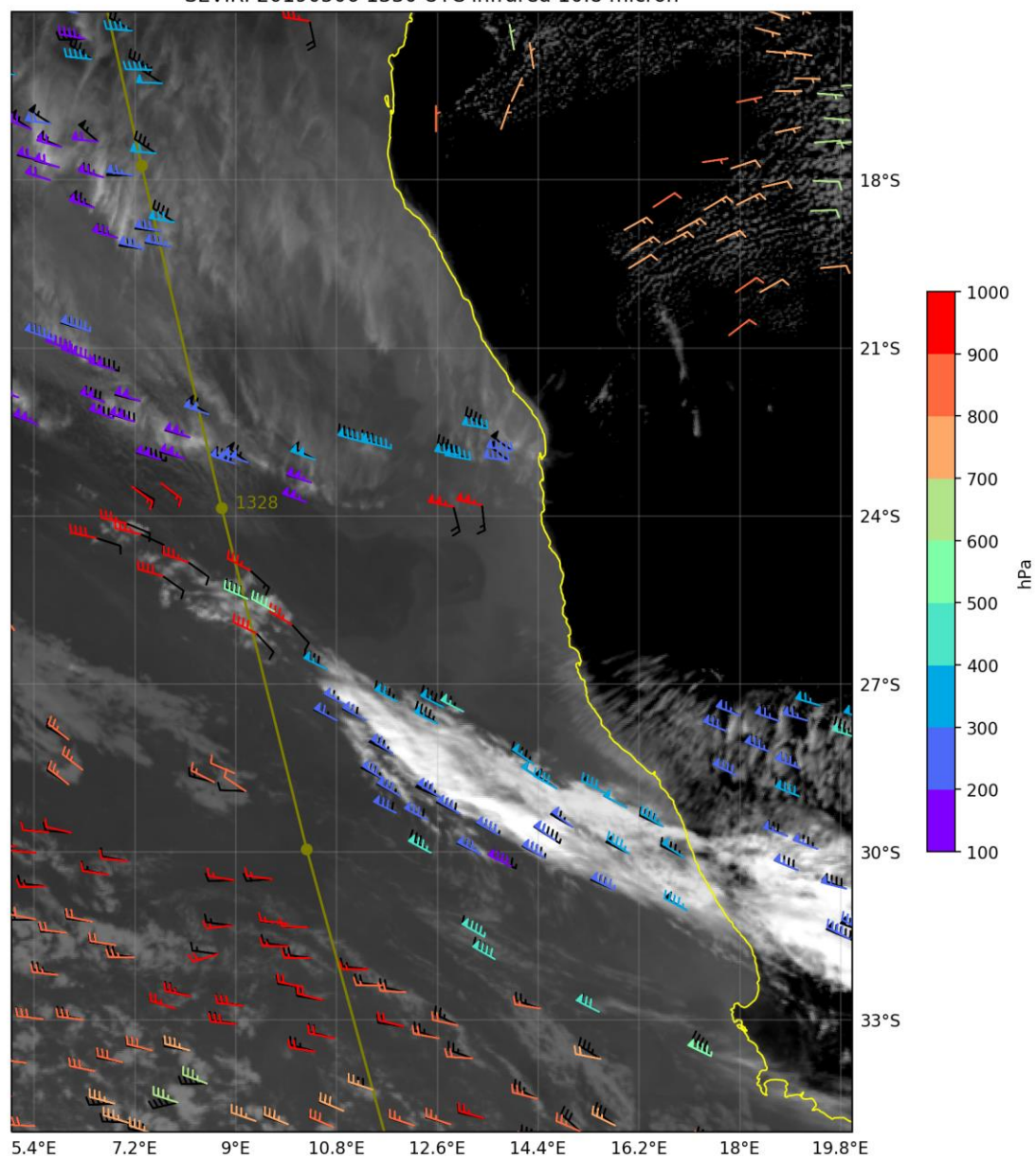


Figure 12. Same caption as Figure 9, but for data valid at 1330 UTC on 6 May 2019. A Calipso overpass at approximately 1328 UTC is plotted as the line with circular markers.

AMV ocam11ir108 20190506T1300Z - 20190506T1400Z
SEVIRI 20190506 1330 UTC infrared 10.8 micron

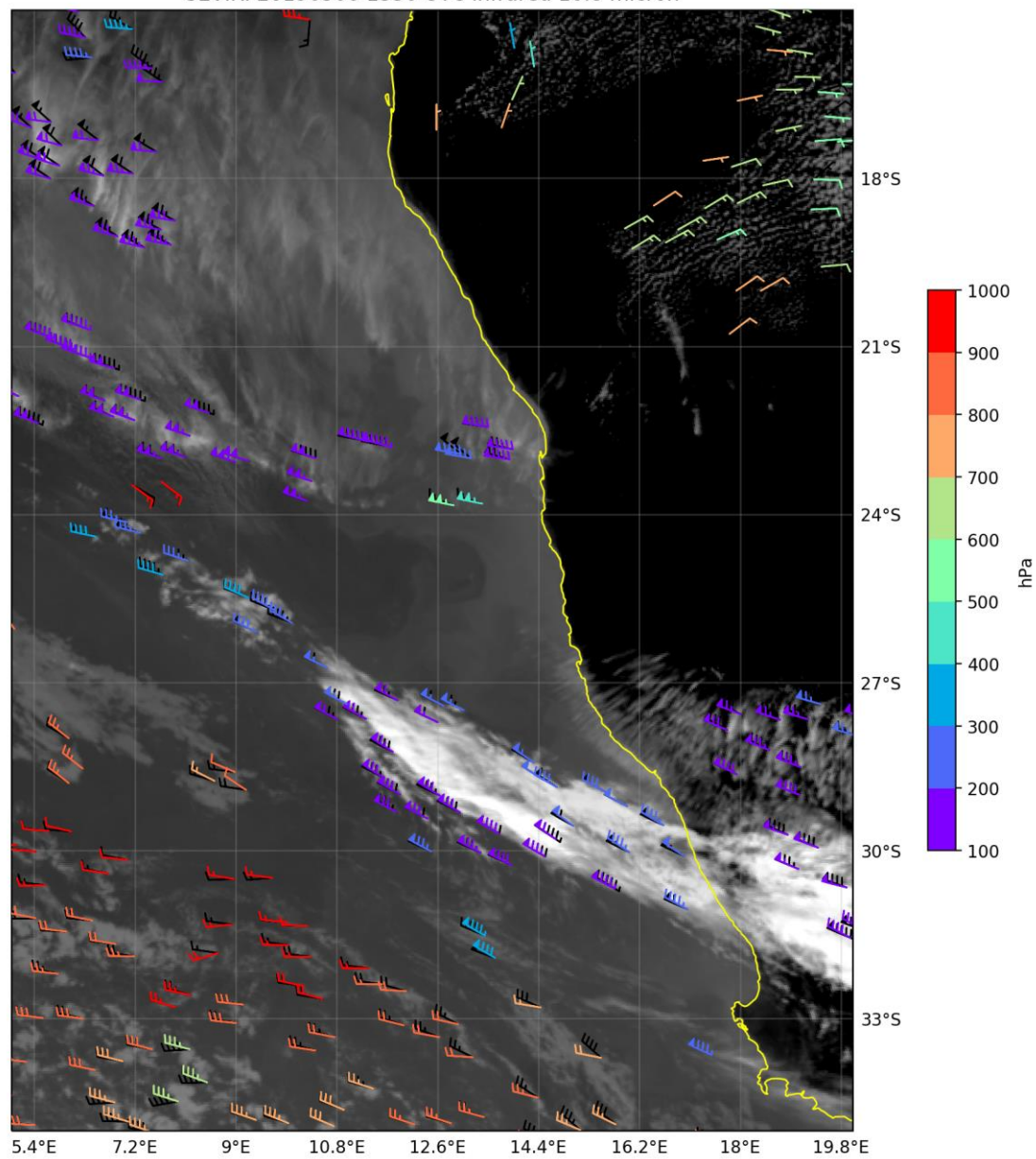


Figure 13. As per Figure 12, but heights from OCA instead of CLA.

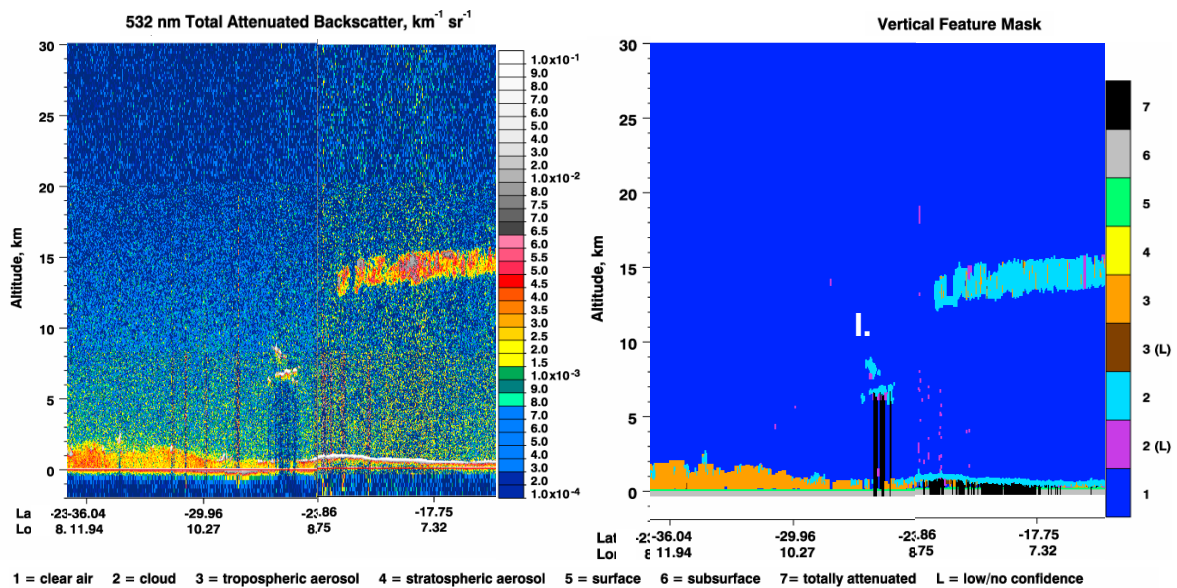


Figure 14. Calipso total attenuated backscatter backscatter and vertical feature mask at ~1328 UTC on 6 May 2019. The Calipso ground track is shown by the line with markers in Figure 12.

6. Feature 9.3: Differences between Met Office and ECMWF statistics for Himawari-8

Zonal statistics for Himawari-8 show noticeable differences between the O-B patterns of the ECMWF and Met Office models.

At upper levels for heights above 400 hPa, but particularly above 200 hPa, O-B mean vector differences (MVD) are consistently lower for ECMWF compared to the Met Office (Figure 15d and Figure 16d). The difference, in excess of 1 ms^{-1} in places, doesn't appear to be linked with a difference in speed bias (e.g. Figure 15a/b). Upper level maps show differences in MVD across large parts of the Himawari disc. Some months show prominent differences around latitude 20°N which appears to be linked to the area of high MVD located around 300-400 hPa (see Figure 16d).

At mid-level in the tropics, between 400-700 hPa, MVD are consistently lower for the Met Office background compared to ECMWF (Figure 15d and Figure 16d). Differences in O-B speed bias at mid-level vary throughout the year. Between approximately June and December, ECMWF have a larger negative speed bias and higher MVD between 400-700 hPa for a region within 10 degrees of the equator (compare Figure 15a/b). Maps indicate this originates from an area east of 140°E over the Pacific Ocean. For the remainder of the year, the Met Office have a larger positive speed bias in the regions around 10°S - 30°S and 10°N - 20°N between 500-800 hPa height (Figure 16a/b).

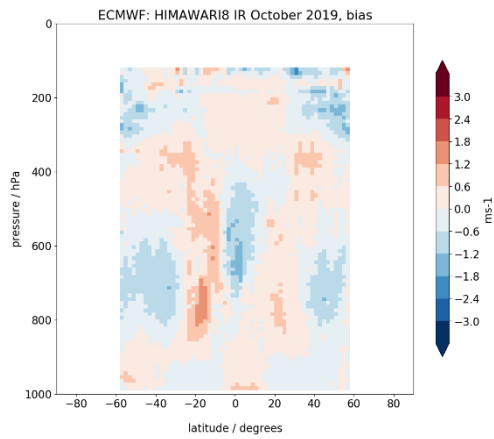
Differences in the way Himawari-8 winds are used in data assimilation could contribute to the differences seen in O-B. The lower MVD between Himawari-8 and the Met Office at mid-level in the tropics could in some part be explained by the stricter spatial quality control employed by ECMWF. In the assimilation, ECMWF reject all Himawari-8 IR winds below 300 hPa in the tropics between 25°N-25°S, whereas the Met Office allows such data to be used. It is therefore expected that the Met Office background will fit closer to Himawari in this region because the observations have been used in forming the analysis. However, ECMWF exclude the mid-level IR data in the tropics not only because of the poorer O-B statistics, but also because of degradation on the impact of short-range forecasts (noted in Lean et al, 2016).

At upper levels, the Met Office reject all above 200 hPa in the extra-tropics and above 160 hPa in the tropics, whereas ECMWF only reject above 150 hPa. This could contribute to the better fit between ECMWF and Himawari above 200 hPa.

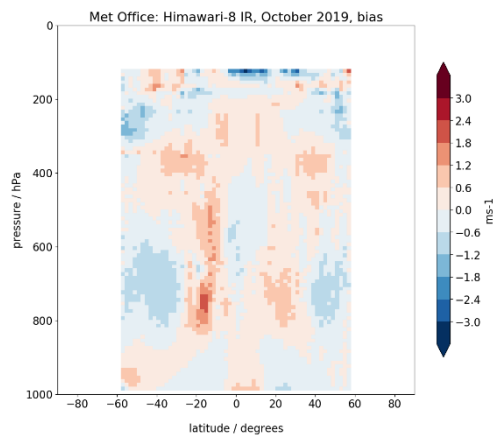
Overall, it is likely that the differences in O-B between Met Office and ECMWF are not solely due to differences in Himawari data use between the centres, but also reflect wider NWP model difficulties in this area.

In December 2019 the Met Office implemented Parallel Suite 43 into operations which included GA7, the latest science configuration of Met Office's global atmosphere model. Early indications show no change in the pattern of differences in MVD between Met Office and ECMWF from this upgrade.

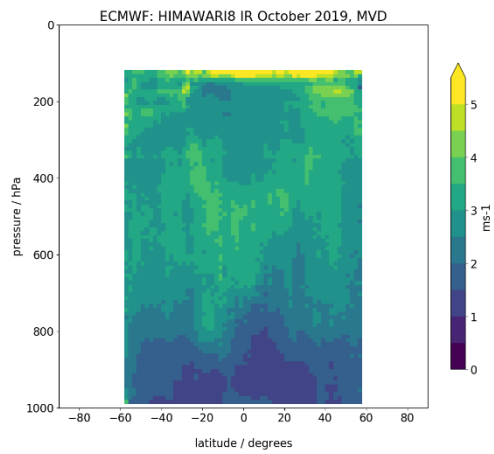
a)



b)



c)



d)

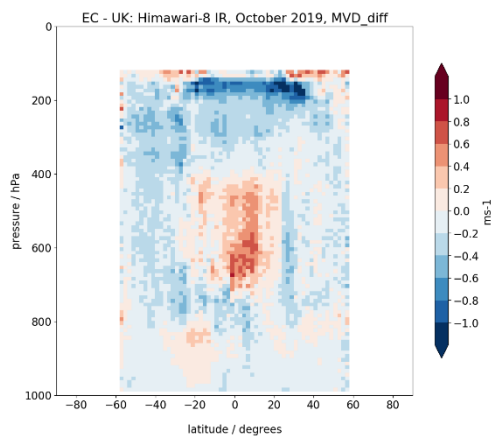


Figure 15. Himawari-8 IR channel O-B statistics as a function of latitude and pressure for October 2019. A) ECMWF wind speed bias, b) Met Office wind speed bias, c) ECMWF O-B mean vector difference (MVD), and d) ECMWF MVD minus Met Office MVD.

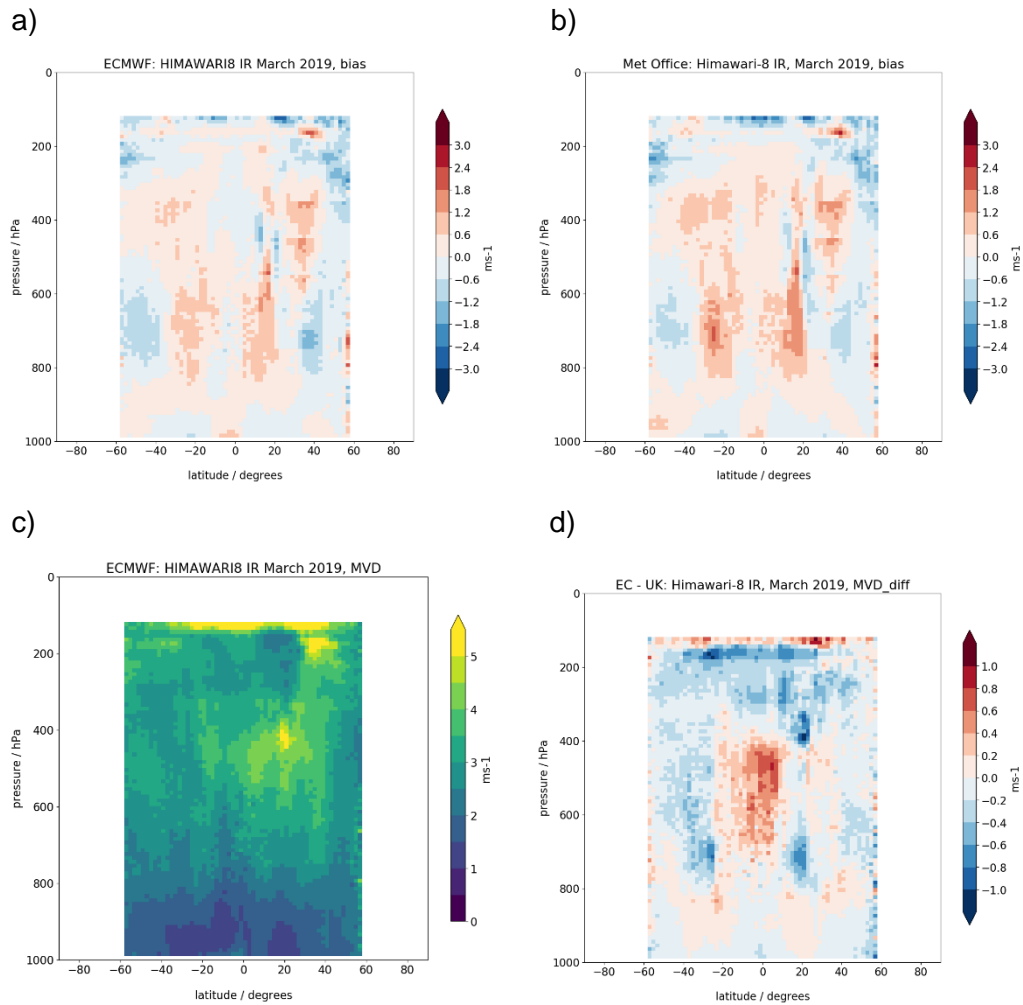


Figure 16. Same caption as Figure 15, but for data in March 2019.

7. Feature 9.4: EUMETSAT Metop low level AMVs in the winter hemisphere

A speed bias and large vector difference is present in EUMETSAT Metop AMVs in the northern hemisphere from Nov to Feb and in the southern hemisphere from May to Sept (Figure 17). This can be seen in the monitoring from 2014-present and is not seen for the Metop winds from CIMSS. It can be seen, but to a much lesser extent because of reduced coverage, in the ECMWF comparison plots.

Case study

The month of November 2019 is selected for further investigation in the northern high latitudes. Examination of the map plots for individual cycles identified the 12 UTC model cycle on 13 November as showing a very strong localised bias over northern Russia.

Further investigation reveals two anomalies in the region located around 123°E and 70°N for AMVs valid at 1019 UTC (Figure 18). The first anomaly is seen around 72°N where observed AMVs slightly inland have high wind speed (30-40 ms⁻¹) but wind directions at 180° to the background. These observations are assigned near the surface (990-1005 hPa) although they match in speed and direction with another area of observations to the east which are assigned to 530-550 hPa. The second anomaly is seen slightly further south, where a strip of AMVs located 68-69°N are assigned to 400-500 hPa. Many observations in this strip are recorded as near zero wind speed, which would be unlikely at this altitude. The background winds at this height suggest wind speeds of 15-20 ms⁻¹. The imagery suggests the AMVs could be erroneously tracking surface features, in this case associated with the contrast between land and frozen river surfaces. There is some evidence of geo-registration errors between the successive image pairs which could be enough to generate a small apparent motion of the surface.

If the same region is examined for the next overpass (Figure 19) both anomalies are reduced. There are no AMVs with near zero wind speeds and most winds assigned very low heights have speeds and directions which agree better with the background.

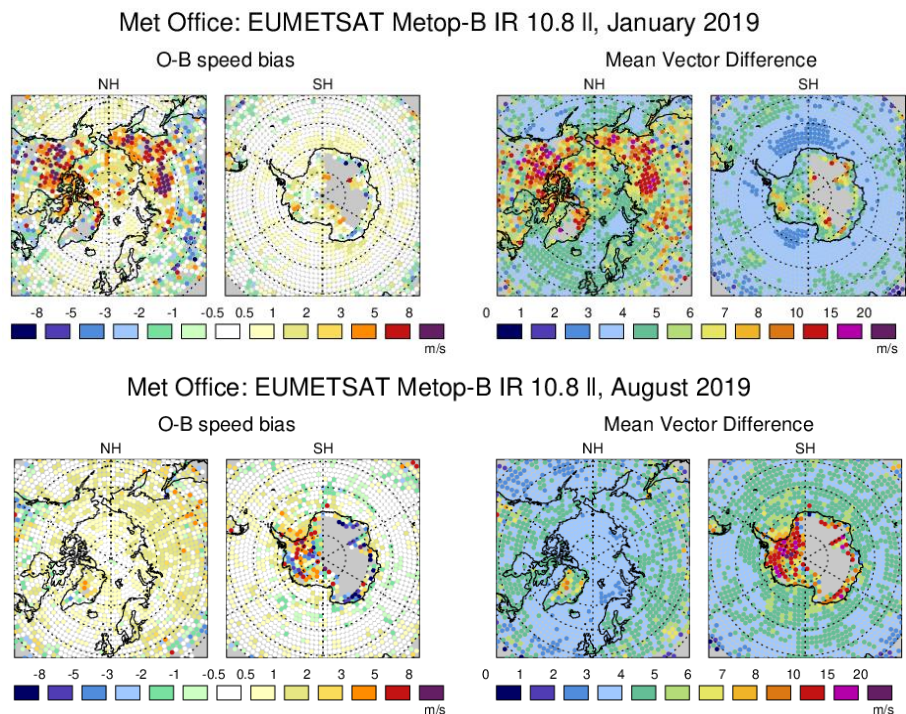


Figure 17. Map of O-B speed bias and mean vector difference for EUMETSAT Metop-B IR channel AMVs below 700 hPa height in January 2019 (top) and August 2019 (bottom).

AMV eumetopair108 20191113T1000Z - 20191113T1030Z
 AVHRR 20191113 1018 UTC Channel 4 Scene radiances

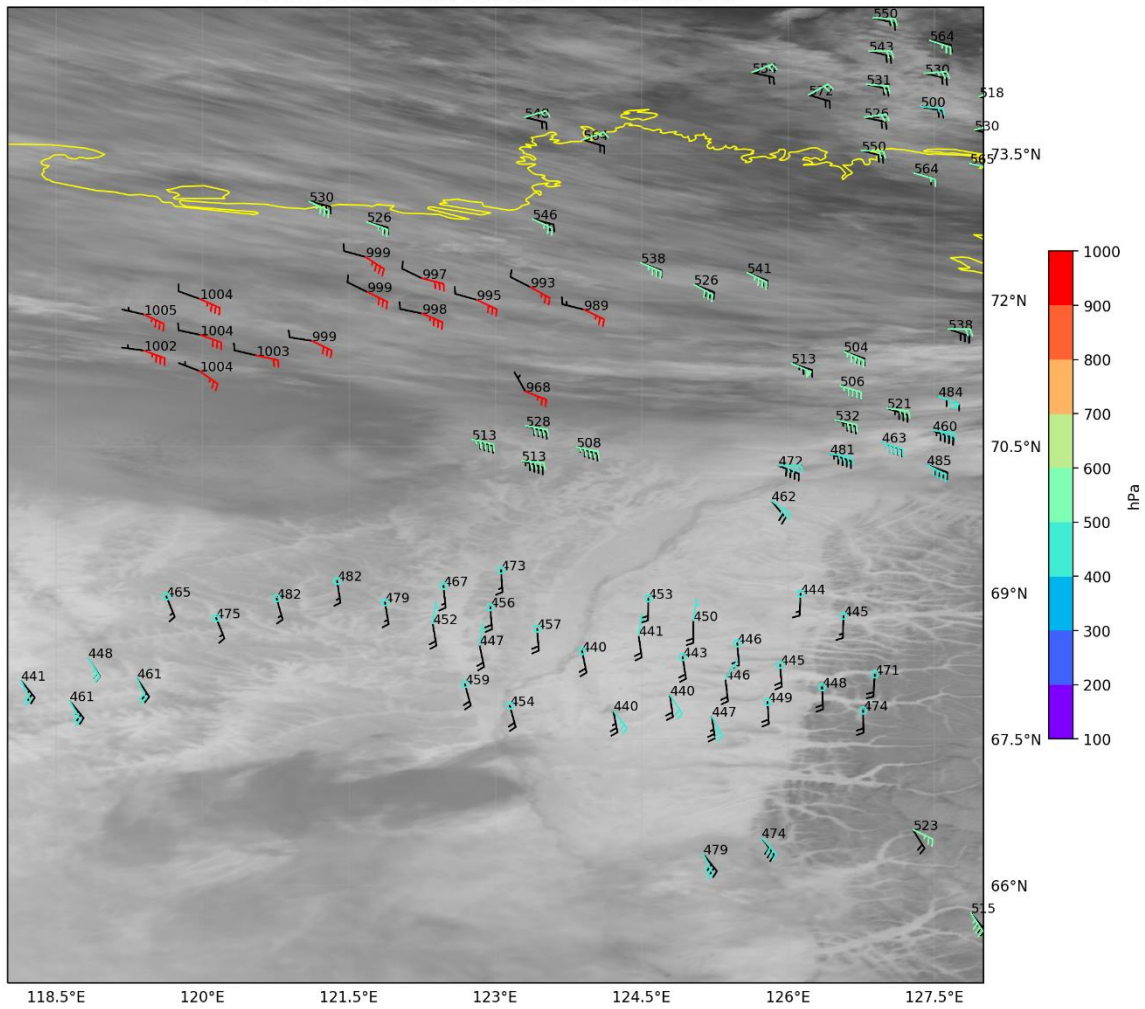


Figure 18. Metop-A IR 10.8µm image and AMVs valid at around 1019 UTC on 13 November 2019. AMV colours represent the assigned AMV height (pressure) band and this is also annotated in black text. Collocated model background winds are shown in black. Half barbs, full barbs and flags represent wind speeds of 2.5 ms⁻¹, 5 ms⁻¹ and 25 ms⁻¹ respectively. The feature running down the image is the River Lena.

AMV eumetopair108 20191113T1140Z - 20191113T1220Z
 AVHRR 20191113 1159 UTC Channel 4 Scene radiances

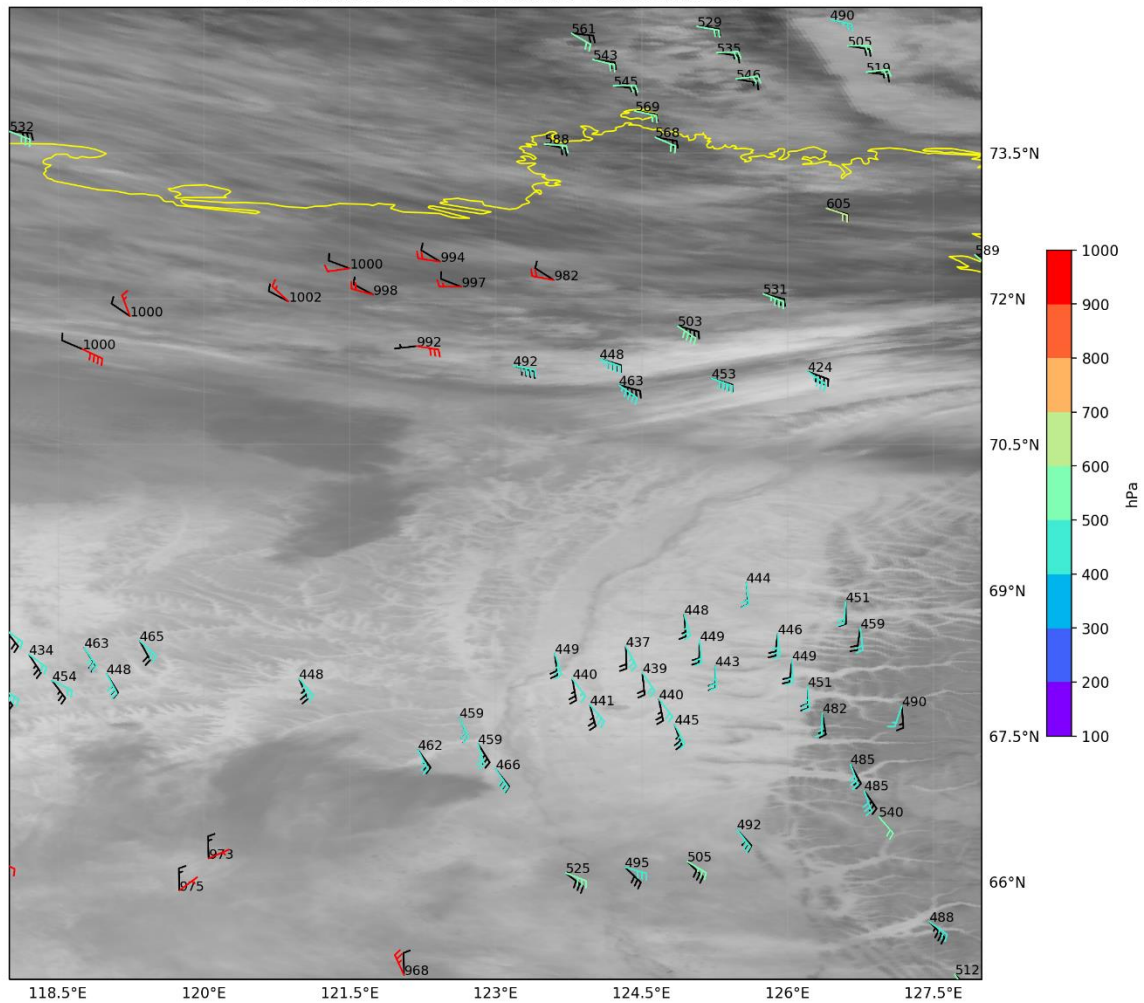


Figure 19. Same caption as Figure 18, but for data valid at around 1201Z on 13 November 2019.

8. Update on Feature 5.2: Meteosat-8/11 negative bias during the Somali Jet

Feature background:

SEVIRI AMVs from Meteosat-8 and Meteosat-10 show a large negative wind speed bias during July and August in the NW Indian Ocean, near the Gulf of Aden. This time period coincides with the strengthening of the Somali Low-Level Jet. Previous investigation has shown the bias is due to instances of height assignment error, with slow upper level vectors incorrectly assigned within the fast, low-level wind regime, and the influence of an island (Socotra) causing semi-stationary wave cloud formations within the jet.

Update:

The monitoring shows that the feature which is so marked in the SEVIRI AMVs is not apparent in the winds from MISR. Matchups of high resolution visible (HRVIS) channel AMVs from Meteosat-8 with MISR show there can be large disagreements in wind speed, direction and height (Figure 20, top). Some matchups have MISR wind speeds at least 10 ms^{-1} faster than Meteosat-8. Wind directions can differ by more than 90 degrees and MISR winds are often assigned to much higher altitudes than Meteosat-8. It should be noted that these differences in vectors and heights do not necessarily relate to the same subset of winds.

The O-B differences at the matchup locations show that MISR vectors are generally in good agreement with the model and the assigned heights correlate very well with model best-fit pressure (Figure 20, middle). Meteosat-8 O-B show an asymmetric wind speed distribution, where AMVs below 10 ms^{-1} have background wind speeds of up to 30 ms^{-1} . Wind directions often differ by around 180 degrees and in many cases the assigned heights are too low (Figure 20, bottom).

Comparison of Meteosat-8 with Calipso lidar heights shows several matchups within the region of the Somali Jet. According to the lidar, many of the AMV heights are far too low (Figure 21). The lidar-AMV matchups show that the tropical Indian Ocean is a frequent source of large height differences.

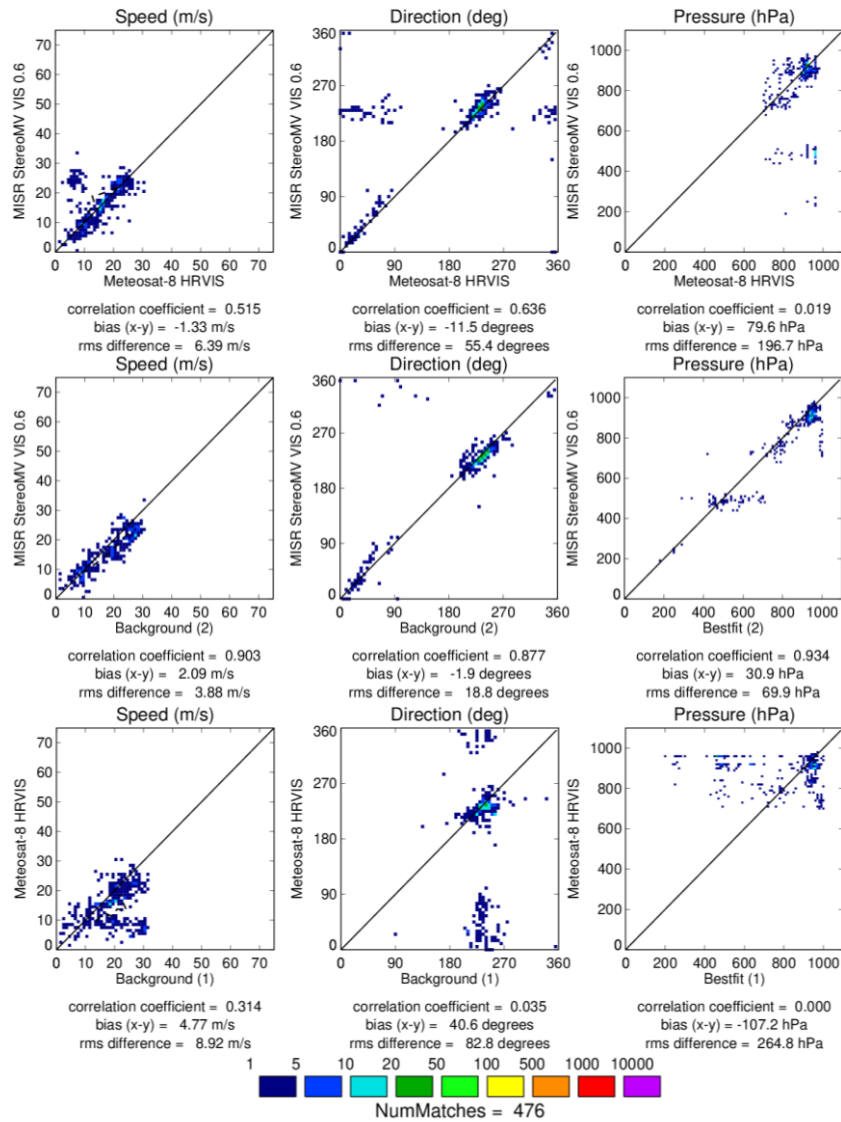


Figure 20. Comparison of Meteosat-8 high resolution visible AMVs, MISR AMVs and the model background. Data from 1-31 July 2019 and filtered for latitude bounds 10N-20N and longitude bounds 50E-62E. Matchups are performed within 10km and 30 mins. Plots show Meteosat-8 vs MISR (top), MISR vs background (middle), and Meteosat-8 vs background (bottom) for comparisons of wind speed, wind direction and assigned pressure.

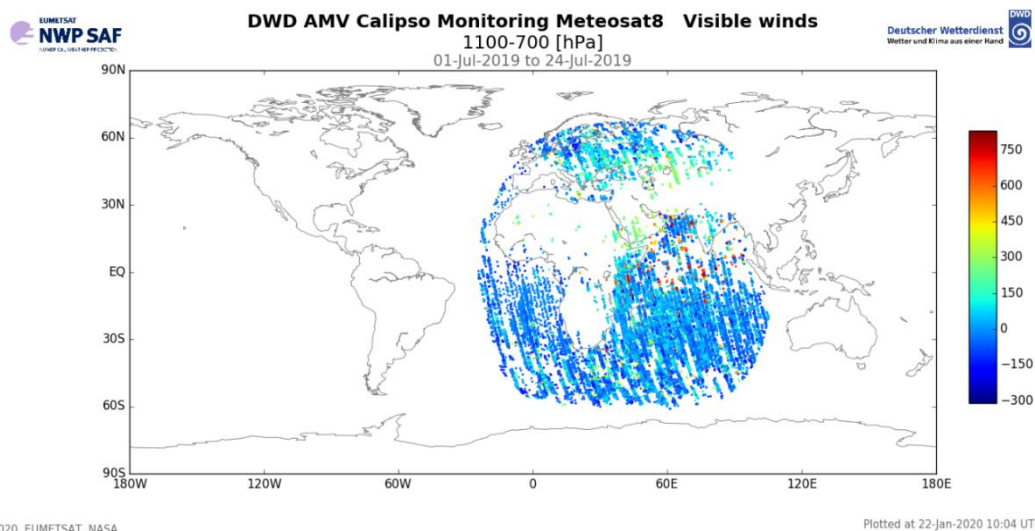


Figure 21. AMV heights minus Calipso height differences for Meteosat-8 visible winds below 700 hPa height. Matchups are for the period 1-24 July 2019.

Case study

The 06 UTC cycle on 8 July 2019 has several matchups between Meteosat-8 and MISR for cases where the Meteosat-8 AMVs disagree with the model. We focus on an area between longitude 59°E and 63°E and latitude 15°N and 18°N. The MISR overpass at 0634 UTC (Figure 22) shows many vectors assigned heights between 960-920 hPa tracking the low-level south-westerly flow. MISR wind speeds are as high as 25 ms⁻¹ for these vectors indicating the presence of a strong low-level jet. MISR also tracks a few brighter clouds which are assigned heights around 480 hPa. These north/north-westerly vectors of around 4-6 ms⁻¹ are slightly slower than the model but wind directions are in good agreement.

Meteosat-8 HRVIS channel AMVs valid at 0630 UTC (Figure 23) show vectors towards the eastern edge of this scene which are also tracking the low-level jet and have similar wind speeds to MISR. For the remainder of the scene however, the Meteosat-8 AMVs show large wind speed and wind direction differences with the model. Focusing on the group of north-westerly vectors near 60.3°E, 16.5°N, we observe that the Meteosat-8 and MISR wind speeds and directions are very similar, but the MISR heights are ~480 hPa and the Meteosat-8 heights are ~945 hPa. Model best-fit pressure for the Meteosat-8 AMVs is near 470 hPa, in good agreement with MISR. OCA heights are missing from the Meteosat-8 data for this period, but we can use Meteosat-11 as a proxy to see if there are any differences to CLA. Although Meteosat-11 tracks fewer vectors here (being near the edge of the disc), the coincident vectors show the same incorrect heights with OCA as Meteosat-8 with CLA.

In this case, when tracking the mid-level clouds, the geometric (stereoscopic) height assignment utilised by MISR is performing much better than the radiometric height assignment used by Meteosat-8.

Another case for the 06 UTC cycle on 13 July 2019 shows MISR vectors again tracking north/north-westerly vectors again around 500 hPa, but background wind speeds are zero or very light from the east/south-east (Figure 24). Model forecast profiles at the MISR locations (e.g. Figure 26) show a layer of very slack winds between around 500-700 hPa. Below this layer the model winds veer with height from a south-westerly near the surface to a westerly. Within the slack layer, wind directions suddenly change to a north-easterly and then easterly. This variability in wind direction is the cause of the discrepancy between MISR and the model.

The MISR winds at 500 hPa are assigned at or just above a strong peak in model humidity, which could indicate the cloud layer being tracked by MISR is at the correct height. In which case it is the model wind profile which is in error. The MISR vectors fit the model best-fit at

around 640 hPa, which suggests the model has the level at which the wind veers around from a westerly to an easterly ~140 hPa too low.

The equivalent vectors from Meteosat-8 for this case are again incorrectly assigned at 960 hPa and 922 hPa (Figure 25).

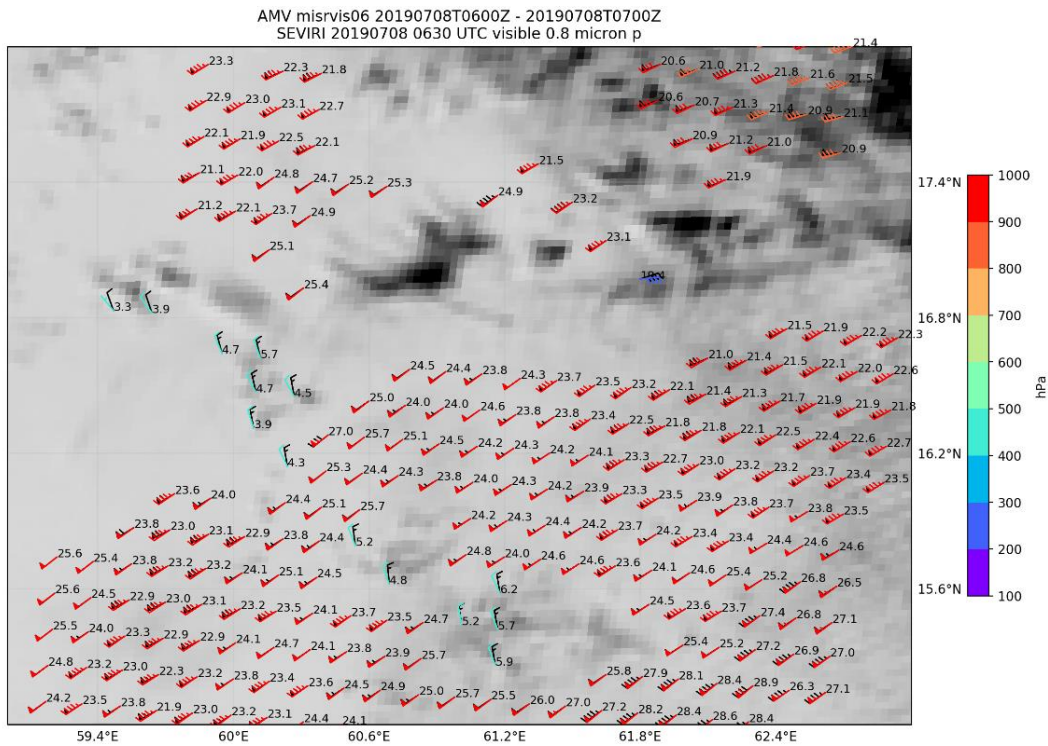


Figure 22. Meteosat-8 visible 0.8 μ m image at 0630 UTC and MISR winds valid at around 0634 UTC on 8 July 2019. AMV colours represent the assigned AMV height (pressure) band. Collocated model background winds are shown in black. Half barbs, full barbs and flags represent wind speeds of 2.5 ms^{-1} , 5 ms^{-1} and 25 ms^{-1} respectively. The AMV wind speeds are also printed beside the vectors. The visible colour scale is inverted for clarity.

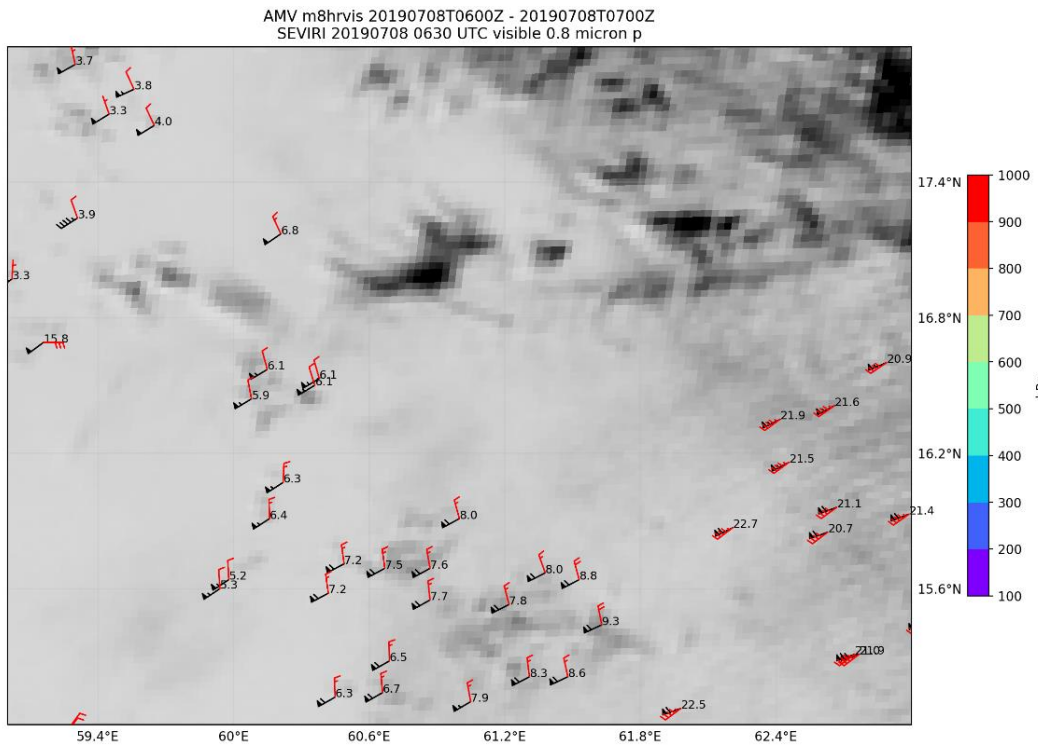


Figure 23. Same caption as Figure 22, but for Meteosat-8 high resolution visible AMVs valid at 0630 UTC.

Sat 3783 VIS0.6 20190713 0654 UTC

lat 12.6 lon 56.0 surf 0 press=508 hPa bfit=636 hPa (T) ep=92 hPa flag 3 qi1=59 qi2=-99
p*=1009 hPa orog=0 m bgRH=77% spd=4.8 m/s bias=2.0 m/s iob 3571

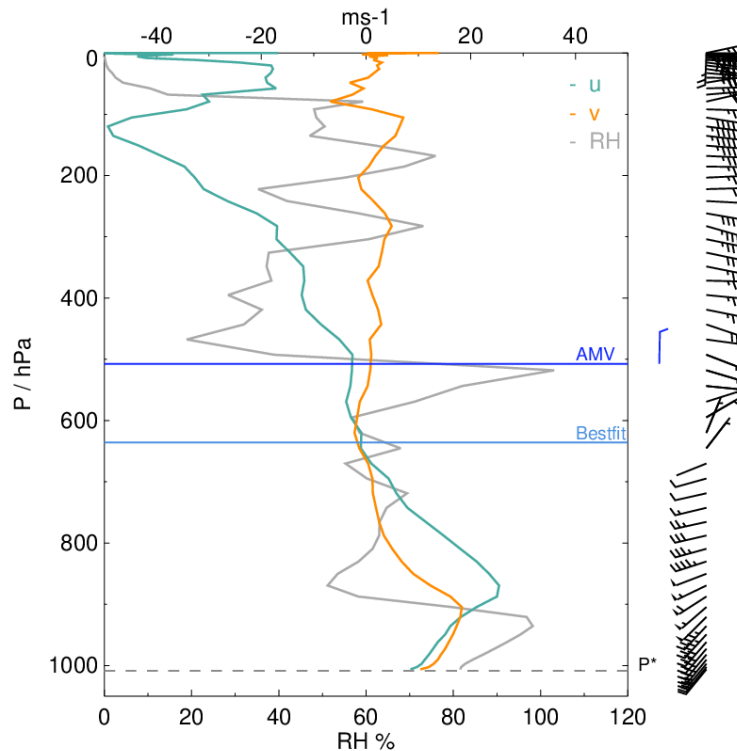


Figure 26. Model profiles of u wind (green), v wind (orange) and relative humidity (grey) for the MISR wind vector located at 12.6N, 56.0E and assigned to 508 hPa in Figure 24. The AMV assigned pressure and model best-fit pressure are shown by the dark and light blue lines respectively. The AMV vector and the profile of model vectors are shown by the wind barbs to the right of the image. Half barbs, full barbs and flags represent wind speeds of 2.5 ms^{-1} , 5 ms^{-1} and 25 ms^{-1} respectively.

9. Update on Feature 8.1: Meteosat-8 (IODC) positive speed difference in the tropics

Feature background:

First reported in AR8, this feature is a bias in low level Meteosat-8 over the Indian Ocean. A positive speed difference and increased RMSVD versus the Met Office and ECMWF model background winds were observed over the tropical Indian Ocean, south of the equator.

Update:

This bias persists, although intensity and coverage are less than in 2017 (see Figure 27 for comparison of changes in bias from August over the three years 2017-2019). The biggest signal seen in the visible $0.8\mu\text{m}$ channel, but it is seen to some extent in the HRVIS and IR channels.

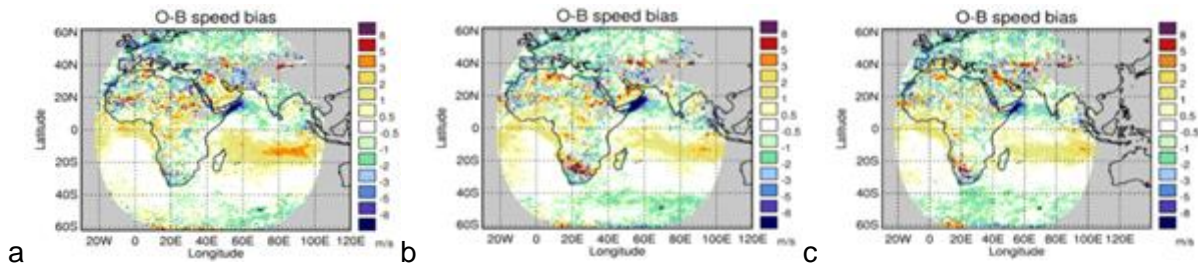


Figure 27. Speed bias for the 0.8 μm visible channel on Meteosat 8 for a) August 2017, b) August 2018 and c) August 2019.

Calipso lidar height matchups indicate that the Indian Ocean region exhibits a different behaviour to other areas. Whilst in general the visible Meteosat-8 winds are assigned lower than the lidar, in the Indian Ocean they are more likely to be too high (Figure 28). The exceptions include cases such as those in Section 8.

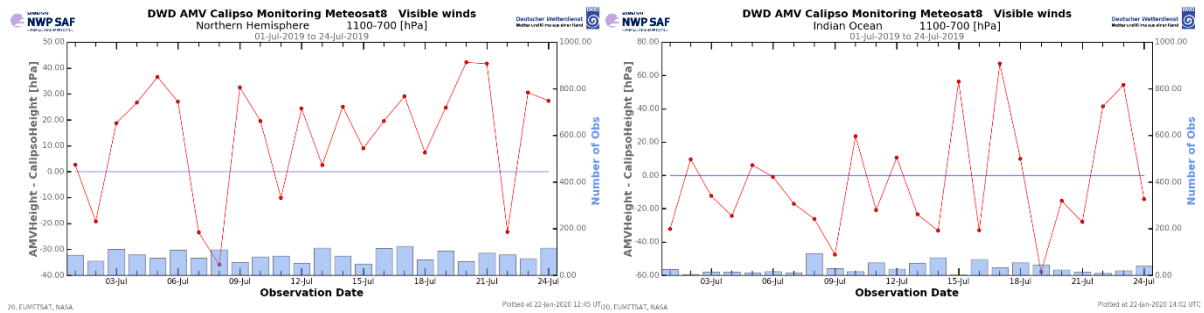


Figure 28. Time series of AMV height minus Calipso height for Meteosat-8 visible winds below 700 hPa height. Matchups are for the period 1-24 July 2019. Northern hemisphere (left) and Indian Ocean (right).

Comparisons with the average Aeolus wind profile and a nearby radiosonde (Cocos Island) show that both agree well with the ECMWF model, supporting the hypothesis that some of the Meteosat-8 AMVs may be assigned too high leading to less wind shear when averaged to give a representative profile. The AMVs show little variation with height compared to the model and both sets of independent observations (Figure 29).

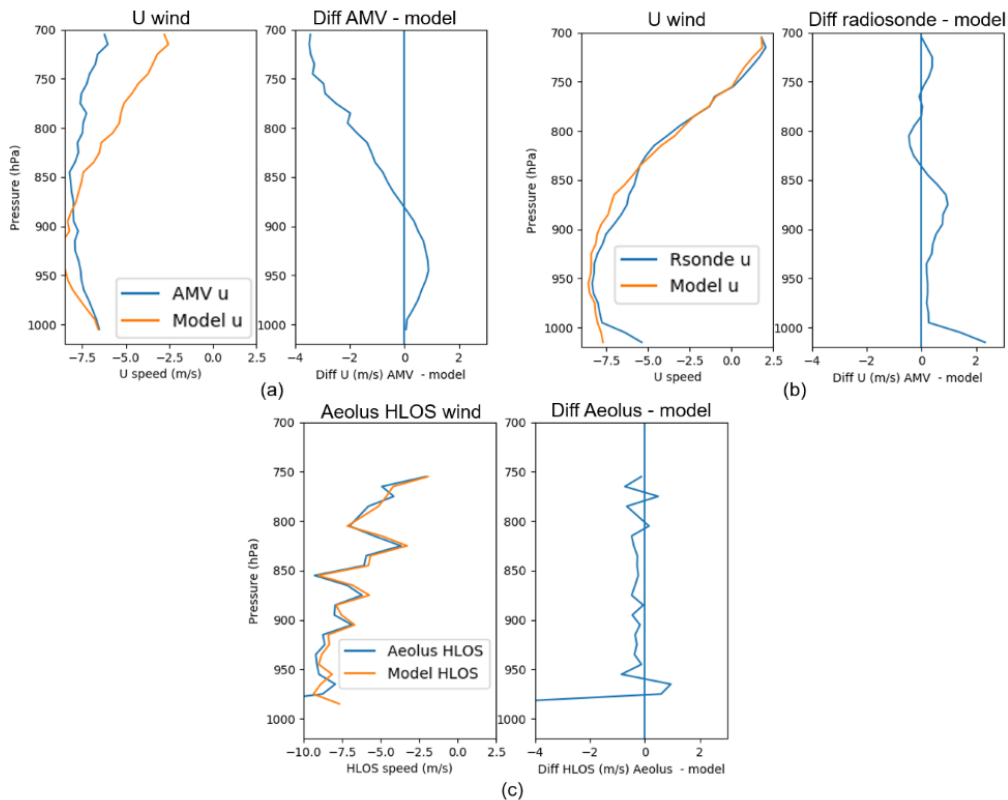


Figure 29. Comparisons with ECMWF model background wind for an assimilation experiment 14 Sept – 13 Oct 2018 and over the area 50-100°E, 5-25°S. a) Meteosat-8 AMVs visible AMVs actively used vs model, b) radiosonde wind profile vs model c) Aeolus wind profile vs model (actively used Aeolus winds, ascending orbits only).

Comparisons with Himawari-8, which overlaps with Meteosat-8 in the area of interest, were also carried out. Collocation of the Meteosat-8 and Himawari-8 AMVs between 600 and 1000 hPa for the month of June 2019 in the region 5-20° south and 80-105° east confirm that Meteosat-8 AMVs are consistently higher in height than both Himawari-8 and model best-fit (Figure 30) throughout most of the pressure range considered. Collocations also show poorer O-B agreement for Meteosat-8 than Himawari-8 at the matchup locations (not shown).

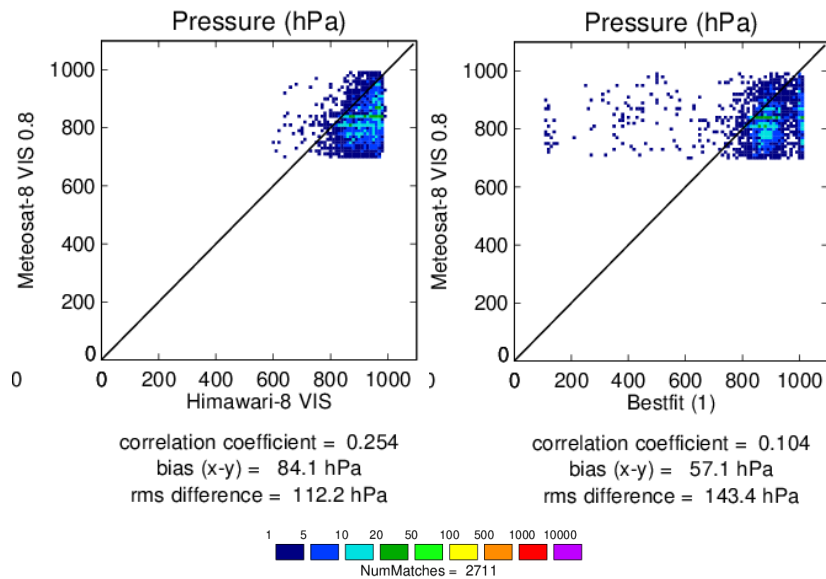


Figure 30. Pressure assignment for Meteosat-8 visible channel against Himawari-8 visible channel (left) and against model best fit pressure (right) for collocated points below 600 hPa height in the region 5-20° south and 80-105° east for June 2019.

The quality of the low level Meteosat-8 winds was also investigated in relation to the placement of the cloud layer in the ECMWF model. AMVs were collocated with profiles of model variables from the first guess (short range forecast from the previous 12-hour cycle) at Tco399 (~25km) resolution and using the closest time step provided at 30-minute intervals. Profiles are given with 137 vertical levels. The cloud layer was estimated using criteria to detect the cloud base used operationally in the Integrated Forecasting System (IFS). Here a cloud layer is defined if:

- cloud liquid water (CLW) or cloud ice water (CIW) exceeds 10-6 kg/kg
- cloud cover fraction exceeds 1%
- At least 3 consecutive model levels meet the first two criteria to provide a layer
- The first layer found above the surface (with cloud top pressure > 700hPa) is used

Statistics were only considered where both the assigned AMV pressure and the cloud top are greater than 700hPa. Although there were spatial and temporal variations, around 80% of AMVs were matched with model profiles identified as containing these low-level cloud layers. Note that there is no claim made here that the ECMWF model cloud is “truth” and some regional systematic errors may exist. However, the model cloud is largely a good estimate with, for example, comparisons of cloud top height and fraction against CALIPSO showing good agreement (Ahlgriem and Köhler, 2010).

The characteristics of the Meteosat-8 AMVs were considered as a function of their placement relative to the cloud layer (Figure 31). This shows that the highest density of Meteosat-8 AMVs do fall within the cloud layer. However, there are also a significant number assigned outside

the cloud. In the corresponding plot of RMSVD the AMVs below the cloud do not show elevated values while those above the cloud show considerably higher values suggesting these might have a more detrimental impact when assimilated.

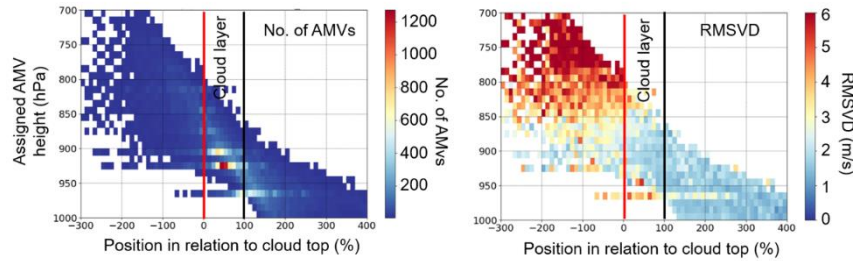


Figure 31. Number of AMVs and RMSVD relative to the model cloud top (<0% = AMV above model cloud, >100% = AMV below model cloud) for Meteosat-8 1st-5th Oct 2018, Tropics region (25°S-25°N), thin clouds (layer < 100hPa) and after screening using forecast independent quality indicator > 85.

Closer inspection of example model wind profiles reveals that at above around 900-950hPa height the AMV is likely in a region of higher wind shear and therefore more sensitive to height assignment errors. For those much closer to the surface, and possibly around the top of the boundary layer, less wind shear could reduce the errors in wind speed. An example is illustrated in Figure 32 which shows the increase in wind shear above the boundary layer top. In this case there are some AMVs which are faster than the model equivalent and placed above where cloud has been diagnosed in the model. Equivalent profiles of the model temperature show that there are inversions present. Potential height assignment errors could also be linked to the misplacement of temperature inversions, but this still requires further study. ECMWF is currently investigating the use of model cloud information as an alternative low-level height assignment method.

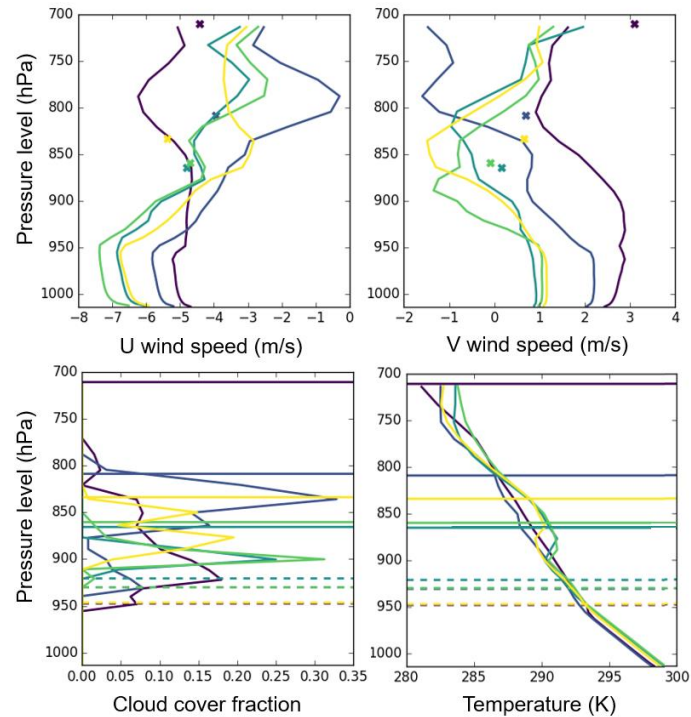


Figure 32. Example model profiles with collocated AMVs from Meteosat-8 at 05Z, 4th Oct 2018, 20-25°S, 65-70°E. Colours are used only to identify the different AMV and model collocated pairs. Crosses in the U/V speed plots (top row) show the AMV values. In the cloud fraction and temperature plots (bottom row), solid lines indicate the assigned height of those AMVs while dotted lines show the corresponding heights of the boundary layer tops for each profile.

10. Summary

This paper marks the ninth iteration of analysis reports for the NWP SAF AMV monitoring. The status of existing features identified in the monitoring has been updated to reflect changes in the past two years. Seven previously active features are now considered closed because the signal is no longer prominent, some of which are related to a change in satellite.

Several new data sets have been added to the monitoring since AR8. These include GOES-16 and GOES-17, which mark a new generation of NOAA geostationary satellites and a new AMV derivation scheme. The gross error check implemented by NOAA/NESDIS in November 2018 has resulted in an improved fit to the model for GOES-16 and GOES-17 AMVs and reduced the bias seen in Features 2.10 and 9.5.

Further investigation for some existing features has expanded our understanding of the cause of the difference between the AMVs and the model:

Update on Feature 5.2: Meteosat-8/11 negative bias during the Somali Jet

The strong negative bias observed for SEVIRI AMVs is not apparent for winds from MISR. We show that in cases where we are tracking mid-level clouds, the geometric height assignment of MISR performs much better than Meteosat-8 which incorrectly assigns these slower winds too low and within the low-level jet. Another case identifies an area of very slack model winds between 500-700 hPa where the wind direction veers very suddenly from a westerly to an easterly. This rapid directional variability causes a discrepancy between MISR vectors and the model.

Update on Feature 8.1: Meteosat-8 (IODC) positive speed difference in the tropics.

Aeolus horizontal line of sight wind profiles show good agreement with the ECMWF model background over the region of interest in the Indian Ocean. Matchups show that Meteosat-8 AMVs are consistently assigned higher heights than Himawari-8 and model best-fit pressure. Both findings support the hypothesis that some Meteosat-8 AMVs are assigned too high leading to less variation of the average wind speed with height. The quality of the low level Meteosat-8 winds was also investigated in relation to the placement of the cloud layer in the ECMWF model. The increase in wind shear above the boundary layer top means that AMVs assigned above the cloud layer are more sensitive to height errors and are found to have considerably higher RMSVD, whilst those assigned below the cloud do not. The role of temperature inversions in these height errors requires further investigation.

In depth investigations have been provided for four new features in AR9:

Feature 9.1: Orographic impacts

AMV biases are considered in the presence of high land surfaces (orography) and we find strong negative speed bias for Meteosat-8 over the Himalayan plateau. There is a consistent 50 hPa height bias between Meteosat-8 and other AMVs in this area, but the corresponding wind speed bias is reduced in the summer months when vertical shear is less.

Feature 9.2: Large vector differences near the South West African coast

Large mean and RMS vector differences are observed near the South West African coast for Meteosat-10 and Meteosat-8. We use case studies to identify two possible causes for the vector differences in this region. Firstly, height assignment errors in the presence of multi-layer cloud, with some improvements seen for OCA heights over CLA in these situations. Secondly, tracking of fog or low cloud motion which is not representative of the local wind regime.

Feature 9.3: Differences between Met Office and ECMWF statistics for Himawari-8

Himawari-8 zonal O-B statistics show differences between the Met Office and ECMWF models. At upper levels, particularly above 200 hPa, MVD are consistently lower for ECMWF, whilst at mid-level in the tropics MVD are consistently lower for the Met Office. The differences in O-B may in part be explained by differences in spatial blacklisting applied to Himawari-8 at the Met Office and ECMWF, but also reflect wider difficulties for NWP models in this region. It is possible that a more consistent use of the AMVs in assimilation would bring the models closer in agreement.

Feature 9.4: EUMETSAT Metop low level AMVs in the winter hemisphere

A speed bias and large vector difference is seen for EUMETSAT Metop AMVs at low level in the winter hemisphere. Case studies identify large height assignment errors for some AMVs assigned near the surface. AMVs with near-zero wind speeds are also identified which are unrealistically assigned to 400-500 hPa. These may result from tracking of surface features associated with the contrast between land and frozen surfaces. There is some evidence to suggest the small apparent motion could be induced by geo-registration errors.

It is hoped the findings of this report will be useful to AMV producers seeking to improve aspects of the AMV derivation schemes, as well as for NWP centres in improving the assimilation and impact of the data. Feedback on the cases investigated in this report are welcome via the NWP SAF helpdesk or directly to james.cotton@metoffice.gov.uk.

11. Acknowledgements

ECMWF statistics are routinely provided thanks to Mohamed Dahoui.

Thanks to Francis Warrick for routinely generating the monthly monitoring plots and maintaining the AMV section of the NWP SAF website.

All EUMETSAT satellite images are copyright © EUMETSAT and are sourced from the EUMETSAT Data Centre:

<http://www.eumetsat.int/website/home/Data/DataDelivery/EUMETSATDataCentre/index.html>

12. References

Ahlgrimm, M., Köhler, M., (2010). Evaluation of Trade Cumulus in the ECMWF Model with Observations from CALIPSO. *Mon. Wea. Rev.*, **138**, 3071–3083, <https://doi.org/10.1175/2010MWR3320.1>

AR8 - Warrick, F., Cotton, J., (2018). NWP SAF AMV monitoring: the 8th Analysis Report (AR8). Document NWPSAF-MO-TR-035. Available from <https://www.nwpsaf.eu/site/monitoring/winds-quality-evaluation/amv/amv-analysis-reports/>

AR6 – Cotton, J. (2014). NWP SAF AMV monitoring: the 6th Analysis Report (AR6). Document NWPSAF-MO-TR-029. Available from <https://www.nwpsaf.eu/site/monitoring/winds-quality-evaluation/amv/amv-analysis-reports/>

Borde, R., Carranza, M., Hautecoeur, O., Barbieux, K. (2019). Winds of Change for Future Operational AMV at EUMETSAT. *Remote Sens.* 2019, **11**(18), 2111. <https://doi.org/10.3390/rs11182111>

Cermak, J. (2012). Low clouds and fog along the South-Western African coast—Satellite-based retrieval and spatial patterns. *Atmospheric Research*, **116**, 15-21.

Daniels, J., Bresky, W., Bailey, A., Allergrino, A., Wanzong, S., Velden, C., (2018). Introducing Atmospheric Motion Vectors Derived from the GOES-16 Advanced Baseline Imager (ABI). 14th International Winds Workshop presentation, Jeju City, South Korea, 23-27 April 2018. Available at http://cimss.ssec.wisc.edu/iwwg/iww14/talks/01_Monday/1400_IWW14_ABI_AMVs_Daniels.pdf

EUMETSAT, 2019. Document: EUMETSAT Product History: 1995-2015, EUM/USC/STD/16/853620 v1A, 31 October 2019. Available from <https://www.eumetsat.int/>

Lean K., Bormann N., Salonen K., (2016), Assessment of Himawari-8 AMV data in the ECMWF system. EUMETSAT/ECMWF Fellowship Programme Research Report No. 42, December 2016. Available from <https://www.ecmwf.int/en/publications>